Fall 10-15-2018

Quantitative validation of simulated sea ice displacements

Bryan R. McCormick
University of New Mexico

Bryan McCormick
Candidate

Mathematics and Statistics
Department

This thesis is approved, and it is acceptable in quality and form for publication:

Approved by the Thesis Committee:

Dr. Deborah Sulsky , Chairperson

Dr. Gunter Leguy

Dr. Helen Wearing

Quantitative validation of simulated sea ice displacements

by

Bryan McCormick

B.S., Biology, University of New Mexico, 2013

THESIS

Submitted in Partial Fulfillment of the
Requirements for the Degree of

Master of Science
Mathematics

The University of New Mexico

Albuquerque, New Mexico

December, 2018

Dedication

For my family and Mel

Acknowledgments

Thank you Dr. Deborah Sulsky, Dr. Gunter Leguy, and Dr. Helen Wearing for your help and support.

Quantitative validation of simulated sea ice displacements

by

Bryan McCormick

B.S., Biology, University of New Mexico, 2013

M.S., Mathematics, University of New Mexico, 2018

Abstract

Accurate simulations of Arctic sea ice are important for forecasting as well as for understanding the global climate. However, quantitative measures for simulation displacements are underutilized. We present five such measures proposed as being useful in the validation of simulated sea ice displacements. Using drifting buoy and satellite measurements of sea ice motion as observation, we apply the metrics in a comparison of observed displacements and predicted displacements from the Arctic sea ice simulation MPM_ice. We find the metric scores are useful for comparing simulations and observations. The metrics also brought to light problems in the simulation MPM_ice, demonstrating their utility in validation of simulated displacements.

Contents

List of Figures

List of Tables

List of Tables

Chapter 1

Introduction

Sea ice is frozen sea water which helps to insulate the ocean from the colder atmosphere in winter and to provide a partial barrier to heat, moisture, and momentum transfer between the ocean and atmosphere, making it an important component in the Earth's energy balance. The ice cover waxes and wanes seasonally and at its maximum extent covers around 7% of the Earth's surface and close to 12% of the Global Ocean [24]. Cracks in the ice cover, called leads, occupy 1-2% of the ice cover in winter but account for half of the heat flux from the ocean to the atmosphere [2].

Accurate simulations of the Arctic are important for commercial reasons, such as transportation, as well as for our understanding of the climate as a whole. A complete description of sea ice requires inclusion of both dynamic and thermodynamic processes. The thermodynamic component should capture heat flux by solving the heat equation through the ice thickness. The dynamic component uses the forces, including wind and ocean drag, the Coriolis force due to the rotation of the Earth, sea surface tilt, and internal forces acting on the ice, as well as the conservation of momentum equations for sea ice to balance changes in the system. Constitutive modeling of ice has evolved over the decades. Nearly all current simulations for

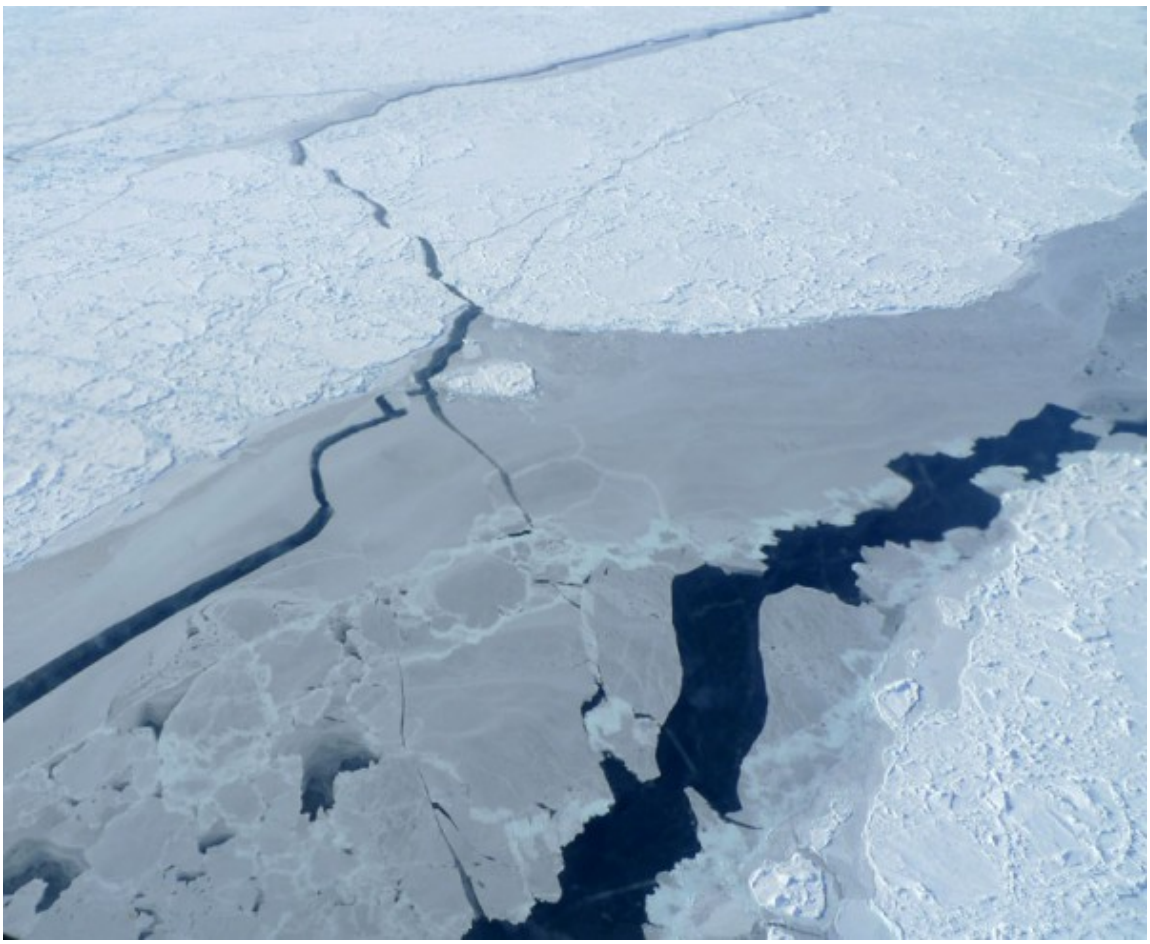

Figure 1.1: Leads near the east coast of Greenland. Photo: Margie Turrin, Lamont-Doherty Earth Observatory.

climate modeling use the viscous-plastic model [11] [12], or a variant, the elastic-viscous-plastic model [13]. These treat ice as an isotropic fluid with variable viscosity. Recent trends in constitutive modeling attempt to account for anisotropies that should be considered when leads are present in the ice [25]. This document will examine displacements predicted by the Material-Point Method sea ice model (MPM_ice) which implements the elastic-decohesive constitutive model for sea ice [19].

MPM_ice uses the Material-Point Method (MPM) to solve the two-dimensional

momentum equation for horizontal motion; a one-dimensional heat equation for thermodynamics in the vertical direction (through the ice thickness), and a balance law for the thickness distribution [22]. MPM uses Lagrangian elements, called material points, to follow the trajectories of ice [22]. The rapid heat exchange between the open water in leads and the Arctic atmosphere, and the reduction of stress after cracking compared to intact ice, play a role in the dynamic and thermodynamic properties of the Arctic and are captured in the model. MPM_ice can model the formation of leads and can predict their widths and orientations [21].

Use of remote sensing, especially via satellites, has provided a wealth of data that can be used to assess the accuracy of numerical simulations of the Arctic. For example, motion data has been derived from high-resolution Synthetic Aperture Radar (SAR) imagery acquired by the RADARSAT satellite. Retrievals from instruments aboard other satellites capture ice concentration and thickness. However, the use of satellites to monitor the Arctic is relatively recent. RADARSAT was launched in 1996, and the data were not processed and published until several years later. Thus, systematic and quantitative assessments of numerical simulations based on these data is still in its infancy.

This thesis will focus on assessing simulated ice motion. For displacement little quantitative analysis has been done with the exception of Grumbine [9], [10]. However, Grumbine's work was limited to the analysis of two older free-drift models. In Chapter 2 we define five metrics proposed in [10] as being useful for the validation of sea ice displacement predictions and in Section 2.6 we present an example of their application to sets of two-dimensional vectors. In Chapter 3 we give an overview of Arctic sea ice motion data used in the comparison to simulation. Chapter 4 presents a comparison between the predicted displacements of MPM_ice and observations for 2001 and 2003. Finally, a discussion of the results and conclusions are given in Chapters 5 and 6, respectively.

Chapter 2

Metrics

In this Chapter, we define the five metrics in [10] suggested for the validation of sea ice displacement predictions, and describe the strengths and weaknesses of each measure. In Section 2.6 we present an example of the metrics' application to simple sets of two-dimensional vectors.

Validation of displacement is difficult because displacement is a vector quantity having both a length and a direction. It should be noted that because the ice extent is much larger than its thickness, ice is modeled as two dimensional. In two dimensions, vectors are described by magnitude and angle. While in sea ice modeling, the statistics of scalar quantities are well studied [18], statistical measures applied to vector quantities remains an area of research. For the purpose of defining the metrics let $(u_{1,i},v_{1,i})$ be a collection of two-dimensional observation vectors with lengths x_i, and angles θ_i; measured counter clockwise from the x-axis in Cartesian geometry. Similarly let $(u_{2,i},v_{2,i})$ be two-dimensional simulation vectors with lengths y_i, and angles ϕ_i. Individual measurements are indexed by $i = 1, 2, ..., n$ where n is the number of observations. We denote by $\bar{u}_j$, $\bar{v}_j$ the means of vector components where $\bar{u}_j = \frac{1}{n}\sum_{i=1}^{n} u_{j,i}$ and $\bar{v}_j = \frac{1}{n}\sum_{i=1}^{n} v_{j,i}$ for $j = 1, 2$. The means of the lengths

and angles of the vectors are defined similarly, with length being the two-dimensional Euclidean norm. We also define the corrected sample covariance between u_i and v_j for $i, j = 1, 2$ by

$$\sigma(u_i, v_j) = \frac{1}{n-1} \sum_{k=1}^{n} (u_{i,k} - \bar{u}_i)(v_{j,k} - \bar{v}_j). \tag{2.1}$$

We define the variance c, as $c = \sigma(z, z)$ and standard deviation as $s = \sqrt{\sigma(z, z)}$, where z may be the components, u_i, v_i for $i = 1, 2$, as well as the lengths or directions of the vector sets. Means of vector lengths or angles will be denoted by μ.

2.1 Error radius

The error radius, R_{err}, is defined as

$$R_{err} = \frac{1}{n} \sum_{i=1}^{n} \sqrt{[(u_{1,i} - u_{2,i})^2 + (v_{1,i} - v_{2,i})^2]}, \tag{2.2}$$

the mean difference between the observation and forecast vector endpoints, with $R_{err} \in [0, \infty)$ and 0 being the best score. This measure is sensitive to both magnitude and direction and a large discrepancy in either will lead to a large error radius.

One drawback is the difficulty in determining whether errors in magnitude or direction are the main contributor to a given score. In other words, identical error radii can be generated by vectors with equal magnitudes in opposite directions or an observed vector with twice the magnitude of the forecast in the same direction.

2.2 Root mean square direction error

The root mean square (RMS) direction error, hereafter direction error, applies the standard scalar RMS error to the difference of angles in radians between forecast and

observed vectors. The direction error, θ_{err}, is calculated as

$$\theta_{err} = \sqrt{\sum_{i=1}^{n} \frac{(\theta_i - \phi_i)^2}{n}} \tag{2.3}$$

For this measure $\theta_{err} \in [0, 2\pi)$ with 0 being the best score.

This metric does not account for the magnitude of the vectors. For this reason the direction error is complementary to the error radius.

2.3 Distance correlation

The distance correlation is the uncorrected sample correlation coefficient for distances x_i and y_i. This metric measures any mutual relationship between the length of observation and simulation vectors regardless of direction.

The distance correlation, ρ, is calculated as

$$\rho = \frac{\sum_{i=1}^{n} x_i y_i - n\bar{x}\bar{y}}{\sqrt{\sum_{i=1}^{n} x_i^2 - n\bar{x}^2}\sqrt{\sum_{i=1}^{n} y_i^2 - n\bar{y}^2}}, \tag{2.4}$$

with $\rho \in [-1, 1]$ with 1 indicating perfect correlation.

One possible disadvantage is that this metric considers the simulation vector length regardless of the magnitude of the observed vector. In other words, a simulation vector length of thirteen-kilometers and observed vector length of three-kilometers will be scored the same as a simulation vector length of forty-kilometers and an observed vector length of thirty-kilometers. The difference in distance is the same but the relative error is not.

2.4 Vector correlation

Vector correlation, described by Crosby in [5], is an attempt to generalize the scalar correlation coefficient to two-dimensions. This metric is a candidate for a universally accepted definition of vector correlation and has several desirable properties. It is a generalization of the square of the simple one-dimensional correlation coefficient and can be interpreted in terms of canonical correlation [5]. Vector correlation is defined as

$$\rho_v^2 = Tr[(\Sigma_{11})^{-1}\Sigma_{12}(\Sigma_{22})^{-1}\Sigma_{21}], \tag{2.5}$$

where $Tr(A)$ is the trace of the $n \times n$ matrix, A. The trace is defined as $Tr(A) = \sum_{i=1}^{n} a_{i,i}$, and the matrices in (2.5) are covariance matrices between observation and simulation vector component sets

$$\Sigma_{ij} = \begin{pmatrix} \sigma(u_i, u_j) & \sigma(u_i, v_j) \\ \sigma(v_i, u_j) & \sigma(v_i, v_j) \end{pmatrix}. \tag{2.6}$$

Equation 2.5 can written as $\rho_v^2 = \frac{f}{g}$, with

$$\begin{aligned} f =& \sigma(u_1, u_1)[\sigma(u_2, u_2)(\sigma(v_1, v_1))^2 + \sigma(v_2, v_2)(\sigma(v_1, u_2))^2] \\ &+ \sigma(v_1, v_1)[\sigma(u_2, u_2)(\sigma(u_1, u_2))^2 + \sigma(v_2, v_2)(\sigma(u_1, u_2))^2] \\ &+ 2[\sigma(u_1, v_1)\sigma(u_1, v_2)\sigma(v_1, u_2)\sigma(u_2, v_2) + \sigma(u_1, v_1)\sigma(u_1, u_2)\sigma(v_1, v_2)\sigma(u_2, v_2)] \\ &- 2[\sigma(u_1, u_1)\sigma(v_1, u_2)\sigma(v_1, v_2)\sigma(u_2, v_2) + \sigma(v_1, v_1)\sigma(u_1, u_2)\sigma(u_1, v_2)\sigma(v_2, v_v) \\ &+ \sigma(u_2, u_2)\sigma(u_1, v_1)\sigma(u_1, v_2)\sigma(v_1, v_2) + \sigma(v_2, v_2)\sigma(u_1, v_1)\sigma(u_1, u_2)\sigma(v_1, u_2)], \end{aligned} \tag{2.7}$$

and

$$g = [\sigma(u_1, u_1)\sigma(v_1, v_1) - (\sigma(u_1, v_1))^2][\sigma(u_2, u_2)\sigma(v_2, v_2) - (\sigma(u_2, v_2))^2], [5]. \tag{2.8}$$

$\rho_v^2 \in [0, 2]$ with 2 being the best score.

Though this metric takes into account both magnitude and direction, by itself it is an insufficient measure for determining how sets of vectors are related. This measure is symmetric with respect to the vector components so a sample of observation and simulation vectors with equal magnitude but opposite directions will give a score of 2.

2.5 Distance Regression Slope

The distance regression slope is the uncorrected covariance between observed and predicted displacement magnitudes divided by the variance of the observed displacement magnitudes. The regression slope, m, is calculated as

$$m = \frac{\sum_{i=1}^{n} x_i y_i - n\bar{x}\bar{y}}{\sum_{i=1}^{n} x_i^2 - n\bar{x}^2}. \tag{2.9}$$

The distance regression slope is not bounded, though 1 is the ideal score.

The distance regression slope gives information complementary to the distance correlation score. If the simulation were consistently off by some factor, α, the correlation coefficient would be one but the regression slope would show the disagreement.

2.6 Metric sensitivity

In order to gain insight into the metrics, we generated a set of vectors from a uniform distribution to serve as a control to which we applied a series of random, but systematically increasing, rotations or dilations. Rotations and dilations were determined by prescribing a maximum of 25 for dilation and 2π for rotation, then to each vector was applied a rotation or dilation from a uniform distribution up to, but

not exceeding the maximum. The altered vectors are then compared to the control. Figure 2.1 shows the scores comparing the experimental and control vectors for the five metrics described in this chapter.

Figure 2.1 (a) shows that the vector correlation decreases monotonically from 2 to 0 with increasing rotation. The direction error and error radius increase with increasing rotation and plateau at values of about 2 and 1, respectively. Both the distance correlation and regression slope show no variation due to change in rotation meaning that they are indicators of changes in dilation.

Figure 2.1 (b) shows increasing regression slope and error radius with increasing dilation. In contrast both vector and distance correlation are decreasing towards 0, though their changes in value remain small after a dilation of 5. Direction error is unaffected by dilation.

Vector correlation is more sensitive to changes in direction compared to changes in dilation, meaning that its interpretation will depend on the direction error score. If we consider that either a dilation of 5 or a rotation of 3 rad is a strong perturbation, then the error radius can be difficult to interpret as its score for each of these perturbations is about 1.

These results illustrate that each metric may not be sensitive to the differences between sets of vectors, but together they can provide a sense of how the sets may differ.

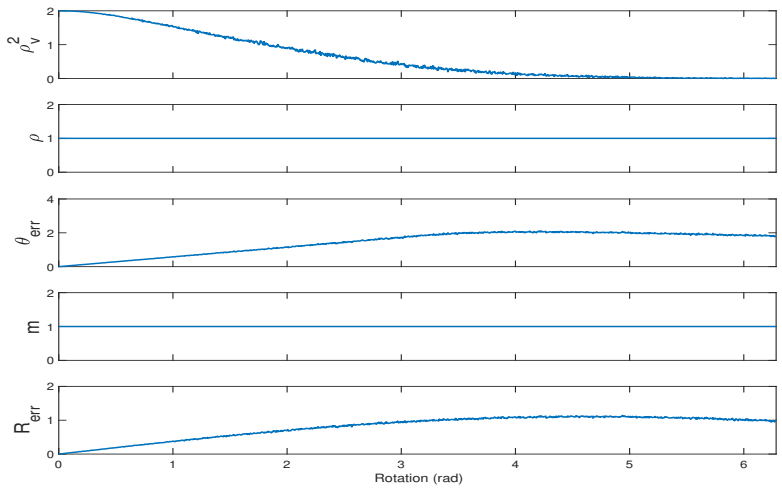

(a) Variable rotations to control vectors.

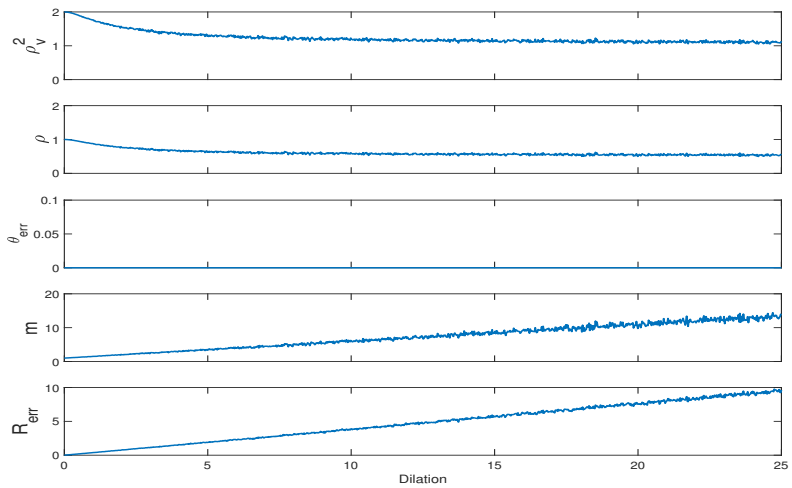

(b) Variable dilations to control vectors.

Figure 2.1: Metric response to systematically increasing rotations (panel (a)) and dilations (panel (b)) of control vectors. In panel (a) as rotations increase, distance correlation and regression slope show no change. Vector correlation decreases with increasing rotation magnitude, while direction error and error radius increase with increasing rotations. In panel (b) error radius shows no response to increasing dilations. Vector correlation and distance correlation decline slowly with increasing dilations. Regression slope and error radius increase linearly with increasing dilations.

Chapter 3

Observation data

This chapter presents an overview of Arctic sea ice motion observations used in the validation of displacements. For this work, observations come from buoys and satellite imagery. While buoy data are more accurate, they do not provide coverage of the entire Arctic Ocean. On the other hand, the satellite data provide coverage over a larger area but with a time gap in the dataset. For this reason, in Section 3.4 we apply the metrics defined in Chapter 2 to the different sets of observation data and show how each dataset can be used for displacement validation.

For processing and applying the metrics the observations are projected to two-dimensional map coordinates. The projection involves polar aspect spherical Lambert azimuthal equal-area projections for the northern hemisphere, described in [20], to transform geographic coordinates to map coordinates using a Matlab function written by Andy Bliss. The projected space is then addressed by an Equal-Area Scalable Earth Grid (EASE-Grid) [4].

3.1 Drifting buoys

One set of observations is generated by the International Arctic Buoy Program (IABP) drifting buoys, made available by the National Snow and Ice Data Center (NSIDC) at http://nsidc.org/data/G00791. Buoys provide real time coverage and move with the ice and for this reason we assume these data to be the most reliable.

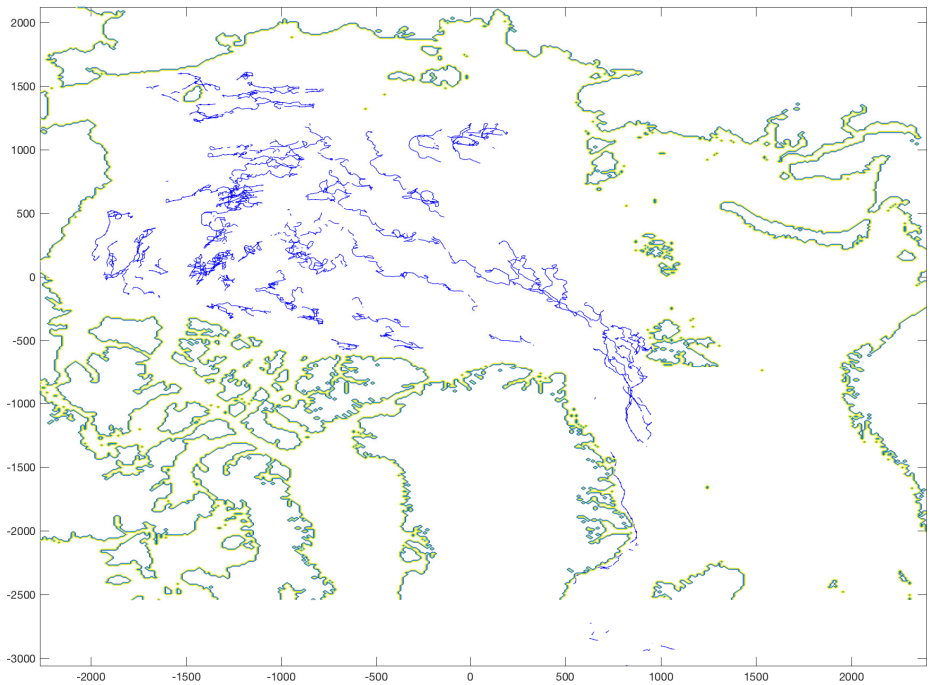

Figure 3.1: Buoy motion for the full year 2003. Buoy trajectories (in blue) are apparent and show the spatial coverage of the data set.

Around twenty-five individual buoys transmit information every twelve-hours. They collect information about the Arctic environment along with their location. The position data files contain the buoy identification number as well as date, time,

latitude, and longitude information. We use the identification number to track each buoy in time and thus its displacement. Figure 3.1 shows all available buoy displacements and trajectories over the full year of 2003.

Though buoys provide very accurate location data, they do not provide coverage of the entire Arctic ocean. For this reason we require an additional data set with coverage where buoy data are scarce.

3.2 RADARSAT geophysical processor system

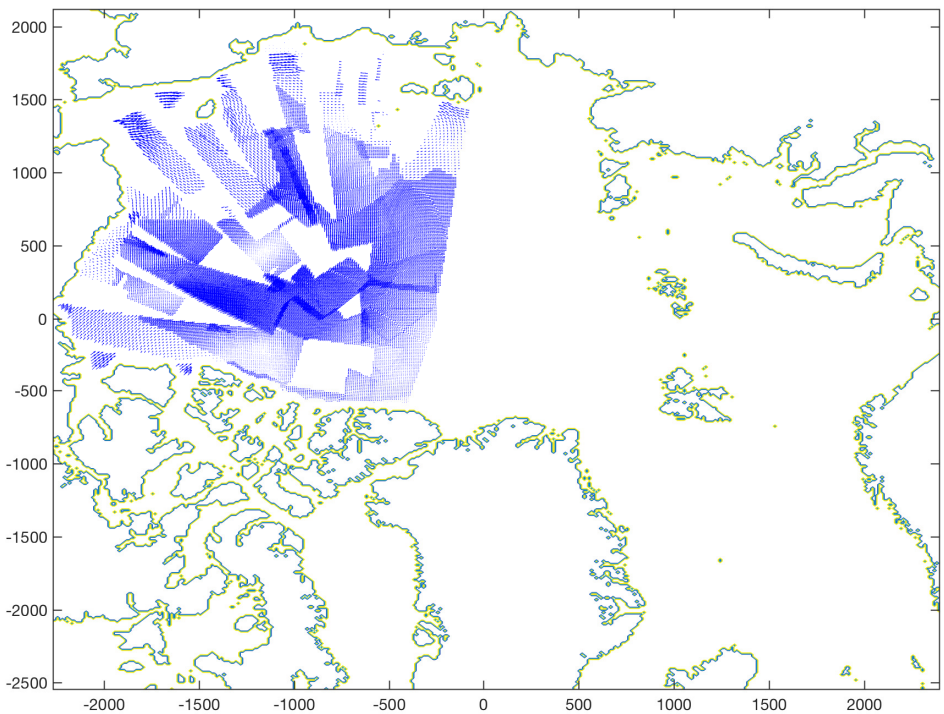

Figure 3.2: Coverage of ASF-RGPS data. Shown are three day displacements for the first three days of January, 2003. Swaths and overlap regions are apparent.

A second set of observations comes from the RADARSAT Geophysical Processor System (RGPS), a NASA funded synthetic aperture radar C-band microwave imaging system, used with the Canadian RADARSAT satellite [14]. RGPS displacements are generated by processing radar backscatter images of the Arctic. Each day the RADARSAT satellite produces an image of a portion of the Arctic in swaths (see Figure 3.2). This process generates an image of the Arctic about every three days and ice displacements are found by tracking features through successive images. One RGPS dataset was obtained from the Alaska Satellite Facility (ASF) at https://www.asf.alaska.edu/sea-ice/sea-ice-data/. The ASF data sets provide Lagrangian trajectories as well as time location and a tracking quality flag associated with the confidence that points in consecutive images are correctly identified.

The ASF data provide very fine spatial and temporal resolution, but the volume of data can limit its usefulness. In order to make these data more accessible, a condensed version was obtained from Ron Kwok of NASA's Jet Propulsion Laboratory in which daily displacements are averaged and interpolated to a uniform 100-kilometer grid (EASE grid described above) for each month of the year. Data were available in this form for 1992 - 2015. An example for January 2001 is shown in Figure 3.3. This data processing allowed for comparisons to be made quickly, and as is shown in Section 3.3, gave information consistent with buoy observations. It is the daily-averaged RGPS, hereafter averaged-RGPS, displacements that are used in the comparison to simulation in Section 4.4.

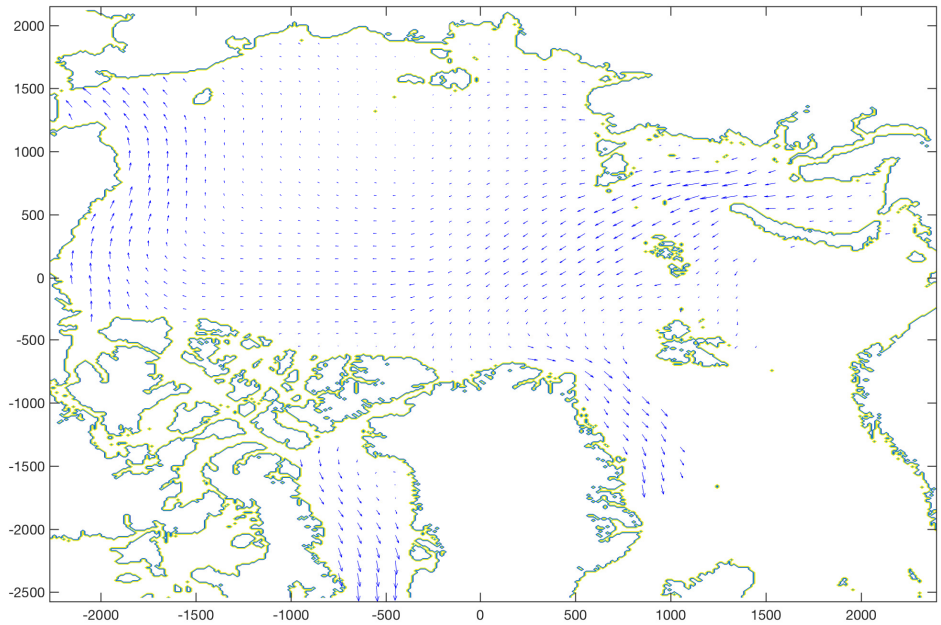

Figure 3.3: Coverage of averaged-RGPS data. Shown are averaged daily displacements for January 2001 interpolated to a uniform 100-kilometer grid (displacement lengths are not to scale). This data set represents a processed form of ASF-RGPS data.

3.3 Observation comparison

We use the metrics defined in Chapter 2 to compare buoy and RGPS displacements in two ways. First, we find the closest averaged-RGPS grid point to each buoy at the beginning of the month, track the buoy for a month, compute its average daily displacement for the month, and compare to the averaged-RGPS displacement at the grid point. Secondly, variable forecast length displacements are compared using the ASF-RGPS dataset by finding the nearest ASF-RGPS point to each buoy and comparing the displacements at the end of the forecast.

3.3.1 Daily average comparison

2003 Averaged-RGPS and IABP Buoy Monthly Comparison						
Month	n	ρ_v^2	θ_{err} (rad)	R_{err} (km)	ρ	m
January	14	1.97	0.151	0.274	0.994	1.03
February	16	1.93	0.235	0.429	0.984	1.07
March	15	1.90	0.357	1.06	0.972	1.73
April	15	1.96	0.411	0.257	0.992	1.02
May	26	1.81	0.280	0.468	0.918	1.15
June	21	1.48	0.264	1.03	0.651	1.33
July	19	1.94	0.193	0.929	0.938	1.34
August	20	1.90	0.267	0.845	0.963	1.11
September	23	1.86	0.245	0.659	0.957	1.17
October	34	1.52	0.566	1.18	0.774	1.23
November	31	1.88	0.263	0.481	0.964	1.04
December	21	1.84	0.185	0.793	0.954	1.02

Table 3.1: Number of available buoys, vector correlation, direction error, error radius, distance correlation, and regression slope for monthly comparisons between averaged buoy and RGPS displacements. Scores show values close to ideal for most months. June and October produced the lowest vector correlation scores and large (relative to this comparison) error radii. The highest direction error occurs in October.

Metric	Score
ρ_v^2	1.77
ρ	0.898
m	1.209
θ_{err} (rad)	0.322
R_{err} (km)	0.730

Table 3.2: Vector correlation, distance correlation, regression slope, direction error, and error radius for 2003 full year comparison of buoy and averaged-RGPS displacements. The annual scores are not representative of the monthly comparisons.

Table 3.1 shows the five metrics for the comparison between averaged-RGPS and daily-averaged buoy displacements for each month of 2003. Vector correlation shows

scores higher than 1.8 for all months except for June and October. In fact, these two months correspond to a strong melt period in the summer and refreeze in winter. It is possible that buoys are not frozen in the ice or that the satellite is unable to track features accurately. However, discrepancies indicated by the metric scores are most likely due to the difference in how the daily averaged displacement at a point is computed. This might explain why October scores the worst for error radius and direction error but has the greatest number of observations. The error radius for March is large as is regression slope and direction error. The scores for regression slope in March, June, and July are larger than the ideal value of 1.

Table 3.2 shows the metric scores for the full year of 2003. However, the annual metrics are not representative of the monthly ones. Vector correlation is lower than 1.8 and the direction error of 0.32 is greater than most of the monthly scores. The annual metric scores might be biased due to outliers or strong seasonal signals (such as melt and refreeze) and for this reason comparisons should be made monthly or over a shorter time span if possible.

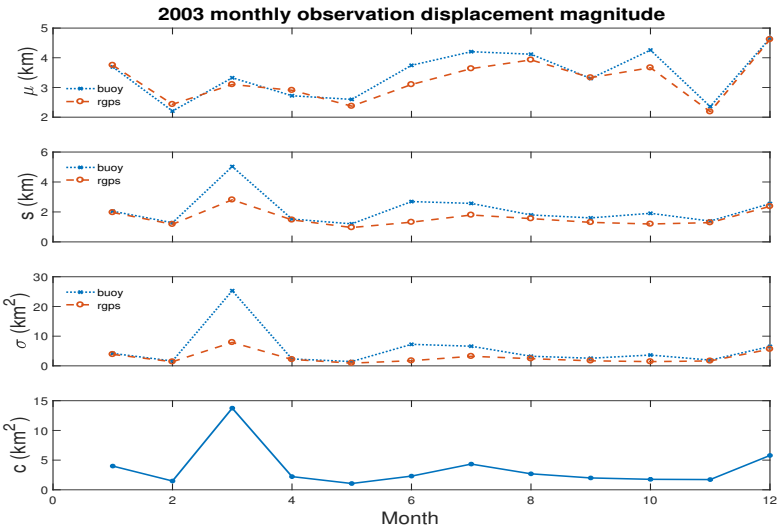

(a) Observation displacement magnitude.

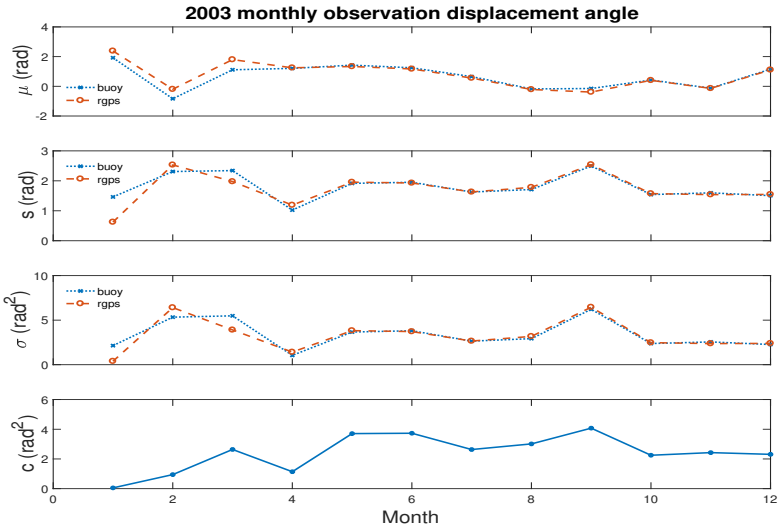

(b) Observation displacement angle.

Figure 3.4: Mean, standard deviation, variance and covariance for averaged-RGPS and buoy displacement magnitudes (panel (a)) and displacement angle (panel (b)) for each month of 2003. Panel (a): Differences in means can be seen in June, July and October, and differences in standard deviations in March, June, and July. These months correspond to periods of strong melt or refreeze. Panel (b): The results are in close agreement suggesting displacement angles are not causing strong discrepancies between the two datasets.

Figure 3.4 (a) shows similar results for the mean, standard deviation, variance, and covariance for daily averaged buoy and averaged-RGPS displacement magnitudes for each month of 2003. Standard deviation and variance are generally higher for the buoys, indicating their displacements take on a wider range of values than those of the averaged-RGPS. The biggest differences in these measures occur in March, June, July, and October which agrees with the results in Table 3.1. The maximum mean displacements for both data sets occurs in December when the ice cover is near its maximum extent. Figure 3.4 (b) shows the mean, standard deviation, variance, and covariance for daily averaged buoy and averaged-RGPS displacement angles for each month of 2003. The results are closer for the displacement angles than for the magnitudes and the biggest differences are seen in the first three-months of the year.

There are several reasons why the scores from the comparison of observation data sets would deviate from ideal values. Worse scores may be expected in the summer when the Arctic ice cover is at a minimum and SAR data are less accurate. This period also coincides with an increase in the formation of leads and break up of pack ice into aggregates which drift freely. Moreover, there is no check implemented to determine whether or not a buoy is frozen in ice. It is possible that some buoys may end up in open water, at which time its displacement no longer reflects the motion of ice. The largest contributor is probably that the average daily buoy displacement is not computed the same as averaged-RGPS. In the former case a single buoy is followed in a Lagrangian sense and its average displacement is obtained along its trajectory. In the latter case, the averaged-RGPS is an average at a fixed point in space.

3.3.2 RGPS, buoy forecast comparison

The temporal coverage of the ASF-RGPS data allows for comparisons to buoy motion with variable forecast length, rather than daily-averages over a month. However, these ASF-RGPS data differ from the IABP buoy location data in that locations are not collected at the same time each day. In order to ensure these time discrepancies do not significantly affect the metric scores, a test is designed to determine the impact of allowing only RGPS location data obtained within a specified amount of time from midnight, the time buoy data are collected.

Figure 3.5 shows the metric scores for a forecast length of six-days for the first 133-days of 2003 between buoy and RGPS data which are filtered by the time of day the data are obtained. The x-axis shows the length of time, in hours, from midnight that an RGPS image is allowed to be used in the comparison. At the point $x = 12$ filtering is no longer applied and RGPS data are considered for that day regardless of the time the back-scatter image is produced. This filtering means that at $x = 3$ only images taken between 21:00, the previous day, and 03:00 are considered, where 00:00 is the start of the day under consideration.

Figure 3.5 shows that time filtering has no affect on vector correlation, distance correlation, or distance regression slope. Error radius increases slightly as the time threshold is increased but drops again when no filtering is applied. Direction error decreases as the time threshold increases with a minimum when no filtering is applied. Time thresholding also decreases the number of RGPS observation points that are available for the comparison.

One possible problem with the test above is that the time thresholding is symmetric with respect to midnight and when the filter is turned off the time frame is no longer symmetric. Whether this asymmetry has any impact on these results is unknown. However, the impact of this time discrepancy should decrease with in-

creasing forecast length. Based on figure 3.5 the metrics suggest that there are no issues with allowing RGPS data to be considered regardless of the time of day the backscatter image is produced, and from this point forward ASF-RGPS data will not be time filtered.

Figure 3.6 shows the metric scores between ASF-RGPS and buoy displacement data for the first 133-days of 2003 with forecast lengths ranging between three and thirty days. The metrics show the observed displacements agree over relatively long periods of time. Error radius remains under 5 km for all forecast lengths. This position discrepancy could possibly be caused by errors in the image processing of RGPS grid points, or by buoys drifting in a lead. Additionally, time filtering (or lack thereof) might also have an impact on error radius. Direction error decreases with increasing forecast length indicating any initial errors become less significant as displacement lengths become larger.

Figure 3.7 (a) shows the mean, standard deviation, variance, and covariance for variable forecast length buoy and ASF-RGPS displacement magnitudes for the first 133-days of 2003. Both data sets closely agree and all the measures increase for both data sets with increasing forecast length.

Figure 3.7 (b) is similar to 3.7 (a) but for buoy and ASF-RGPS displacement angles for the first 133-days of 2003. RGPS has a slightly higher mean angle for nearly all forecast lengths. For a forecast length of fifteen days the mean buoy displacement angle is larger than that of the RGPS. This forecast length also corresponds to the maximum of the standard deviation, variance, and covariance of both data sets.

A similar comparison between buoy and RGPS displacements is made in [17] for forecast lengths up to twelve days. The comparison uses a metric which is the square of the distance correlation coefficient implemented here, and the score in [17] of 0.996 is consistent with the scores obtained here of 0.992 for a forecast length of

twelve-days. Another measure implemented in [17] is the root mean square difference of magnitudes. This metric should be similar to the error radius defined in Chapter 2 though the directions of the displacements are not considered. Lindsay and Stern [17] found a root mean square difference of 1.4 km for forecast lengths up to twelve days, which is smaller than the error radius scores obtained here at close to 3 km.

The comparison between the two sets of observations gives confidence that the metrics will give reasonable scores when comparing related sets of vectors. This property is desirable for metrics used in model validation. Therefore, if the metrics give good scores in the comparison of vectors predicted by a simulation to observed displacement vectors, one can conclude the sets of vectors agree and that the model is performing well.

3.3.3 Inter-comparison of RGPS data

In this section we apply the metrics in a comparison of the ASF and averaged-RGPS datasets.

Table 3.4 shows the metric scores for the inter-comparison of ASF and averaged-RGPS displacement data. The two sets closely agree and show the data sets are consistent. To make the comparison, for each of the averaged-RGPS grid points is found the nearest point from the ASF-RGPS data set. If no point is found within thirty kilometers the grid point is excluded from the comparison. Daily displacements are computed and averaged for the point from the ASF dataset in the same manner as is done for buoys and compared to the averaged-RGPS displacement. Because the averaged-RGPS is a processed form of the ASF-RGPS dataset the comparison should give a sense of the errors introduced in the processing of the data. February scored worst in vector correlation, distance correlation, and regression slope, though it scored well for error radius. Other scores are close to their ideal values.

Metric	Score
ρ_v^2	1.86
ρ	0.919
m	0.794
θ_{err} (rad)	0.413
R_{err} (km)	0.651

Table 3.3: Metric scores for the January through April, 2003 inter-comparison of ASF and averaged-RGPS displacement data. Metric scores show some discrepancies between the datasets, particularly regression slope and direction error.

Table 3.3 shows the metric scores for the first 133-days of 2003. These results should inform how the metric scores are interpreted in the validation of displacement predictions.

Comparison of Monthly Averaged and ASF-RGPS Displacements						
Month	n	ρ_v^2	θ_{err} (rad)	R_{err} (km)	ρ	m
January	80	1.82	0.644	1.06	0.910	1.00
February	191	1.81	0.360	0.588	0.870	1.12
March	33	1.90	0.466	0.634	0.899	0.963
April	100	1.88	0.199	0.449	0.960	1.02

Table 3.4: Number of observations, vector correlation, direction error, error radius, distance correlation, and regression slope for comparison between averaged and ASF-RGPS data for January through April, 2003.

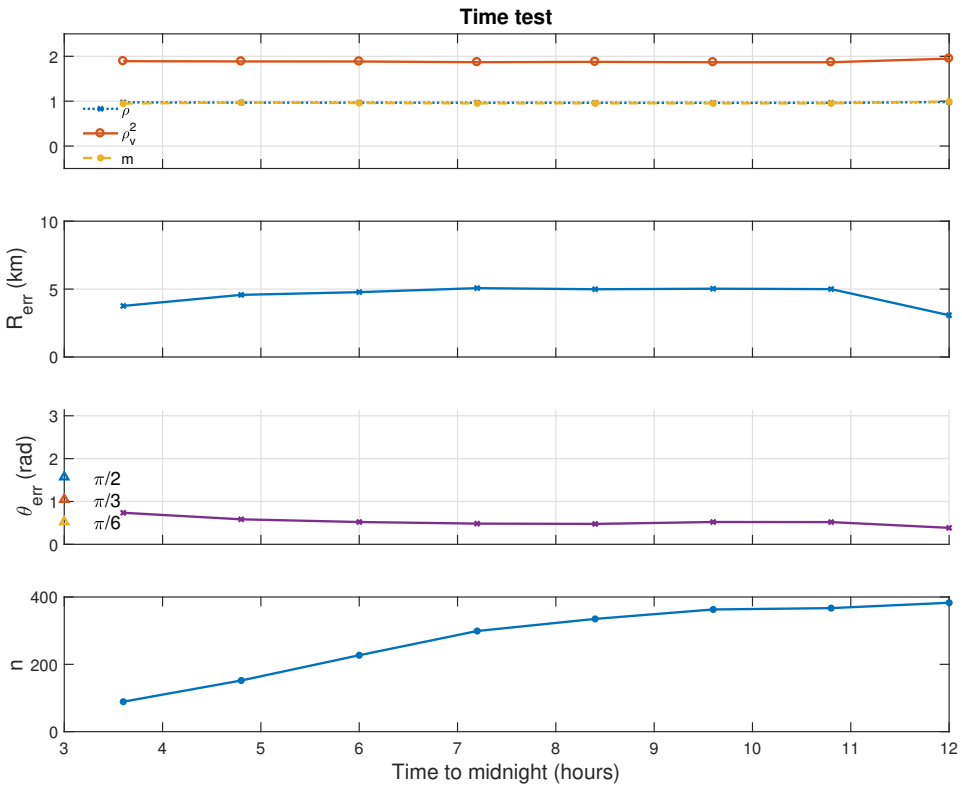

Figure 3.5: Vector correlation, distance correlation, regression slope, direction error, error radius, and number of observations available for time filtered ASF-RGPS displacements compared to buoy displacements with a forecast length of six-days. Data from the ASF-RGPS data set are only considered if the backscatter image, from which the data are generated, was taken within a specified length of time from midnight (shown on the x-axis). The results show that time filtering does not significantly affect the metric scores.

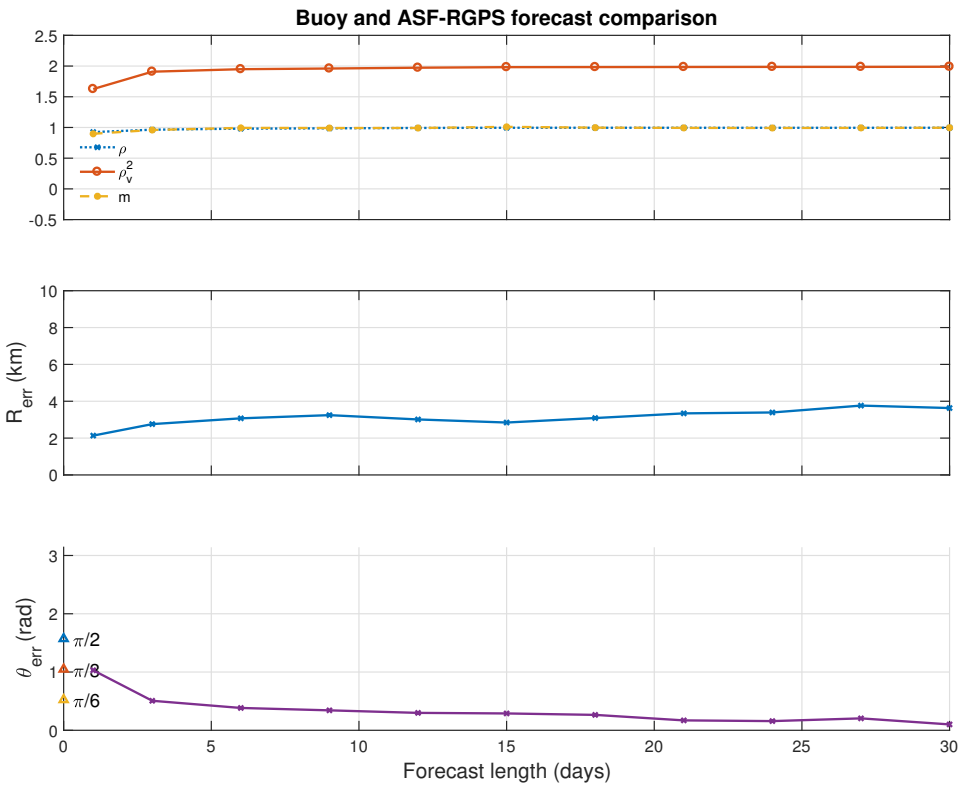

Figure 3.6: Vector correlation, distance correlation, regression slope, direction error, and error radius for the variable forecast length comparison between ASF-RGPS and buoy displacements for the first 133-days of 2003. Scores are slightly worse for one day forecast, which may be explained in part by the difference in the way averaged daily displacements are computed between the data sets. Error radius is large throughout the comparison, possibly caused by discrepancies in the satellite data, or buoys in open water. The other four metric scores are close to ideal values.

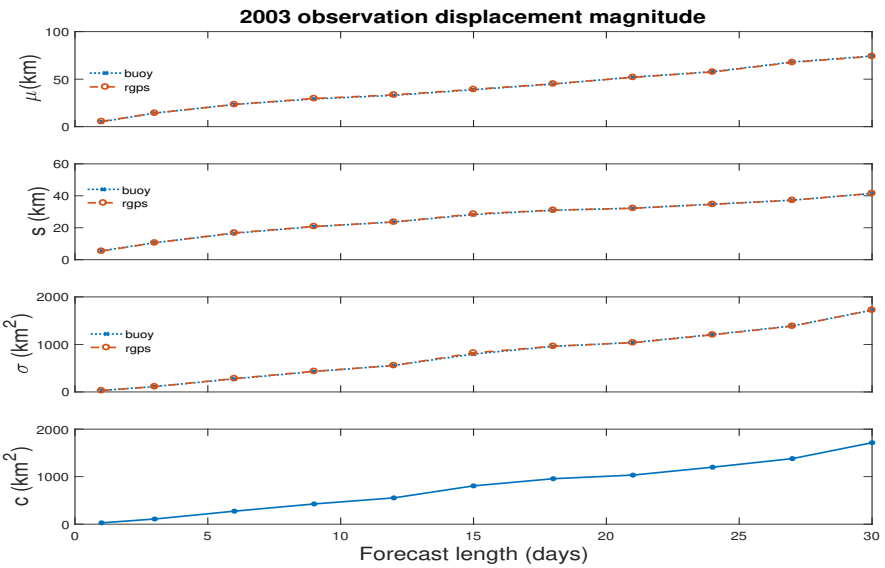

(a) Observation displacement magnitude.

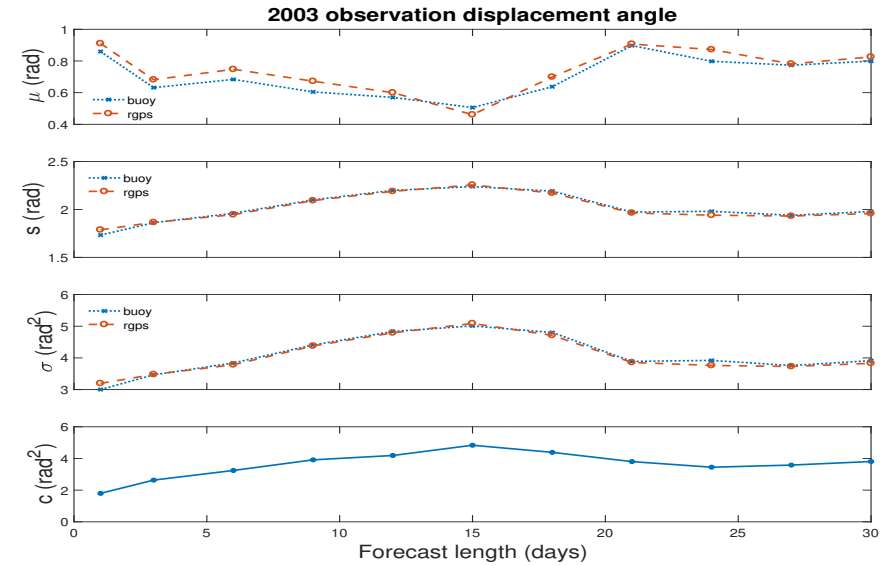

(b) Observation displacement angle.

Figure 3.7: Means, standard deviations, variances and covariance for buoys and ASF-RGPS displacement magnitudes (panel (a)) and angles (panel (b)) for variable forecast length displacements for the first 133-days of 2003. Displacement statistics agree for the data sets with increasing forecast length. Mean displacement angle differs slightly between the two datasets.

Chapter 4

Results

In this Chapter we present an overview of MPM_ice and compare simulated displacements with observations described in the previous chapter. We show a comparison of variable forecast length using drifting buoy data in Section 4.3, as well as a comparison of averaged daily displacements for each month using averaged-RGPS displacements in Section 4.4. In this chapter we denote the difference of displacement statistics by Δ, where the difference is taken relative to the observation. For example the difference in displacement means is denoted by $\Delta\mu = \mu_{obs} - \mu_{sim}$, where μ_{obs} is the observed mean displacement magnitude and μ_{sim} is the predicted mean displacement magnitude.

4.1 Simulations

The simulation data were provided by Deborah Sulsky in the form of netcdf files. Though the simulation generates information about many aspects of the Arctic environment, only displacements are considered here. In the simulation, sea ice is represented by discrete points, called material points (MPs), which are created and

tracked throughout the simulation [22]. MPM_ice is coupled to the Massachusetts Institute of Technology General Circulation Model (MITgcm) ocean code which solves the Boussinesq, incompressible hydrostatic primitive equations [1]. The coupling is two-way with fluxes between the ocean component of MITgcm and MPM_ice serving as boundary conditions between the ice and ocean simulations.

Due to the large size of simulation files, MP data are accessed only for the start and end day of each forecast period. Each MP is associated to an initial position and a possibly non-unique identification number, due to the use of the same ID numbers on different processors. Taken together these data uniquely identify each MP while it exists in the simulation. Before comparing to observations, simulation data are converted to spherical latitude and longitude coordinates and then stereographically projected into the same two-dimensional space as the observation data. Based on the observation data, MPs with the closest straight line distance to each available observation point's initial position are found and stored. If the same MP exists on the forecast end day its position is stored and displacements are calculated based on the initial and final positions. Some MPs may melt in the simulation before the end of the forecast period, and to these points is assigned a displacement of zero for comparison, regardless of when during the forecast period the point melted. At the end of the forecast period the displacement vectors are saved and the process is repeated with the metrics being applied at the end of the period being examined.

4.2 Comparison of buoys and MPM_ice

Comparisons with buoys are done for three-month periods, January through March, April through June, July through September, and October through December for 2001 and 2003. Comparisons with buoy data can be made with a specified forecast length, where the displacement is taken to be the position at the end of the forecast

period minus the position at the start. For the purpose of this work, each buoy is compared to a single MP with the shortest straight line distance to the buoy. Observation and simulation starting points do not coincide exactly but are generally less than 5 km apart. If the closest simulation point to any observation is greater than 30 km then both observation and simulation points are excluded from the comparison.

Comparisons between buoys and forecast displacements are made with forecast lengths from one to thirty days. Longer forecast lengths were examined but proved less reliable. Sorted buoy data are accessed based on forecast start and end date. For buoys with available data, displacements are computed and stored until the end of the three-month period.

4.2.1 2001

Figure 4.1 shows the metric scores for all comparisons to buoys made for 2001. January-March, in black, and October-December, in blue, produced near constant direction errors for the duration of the comparison. Error radius scores for these months increases linearly with increasing forecast length, which is consistent with near constant direction error. These measures together indicate that simulation and observation are drifting apart through time. Distance regression slope for January-March is greater than one for forecast lengths longer than five days with high distance correlation, suggesting the variance of the displacement magnitudes is too large in the simulation. Distance regression slope and correlation for October-December are both close to one-half indicating observation and simulation displacement magnitudes are not well correlated during this time. Smaller errors in direction predictions contribute to higher vector correlation scores for October-December, while smaller errors in magnitude predictions contribute to higher vector correlation scores for January-March.

Similarly, direction error scores for April-June, in green, and July-September, in red, are close to constant throughout the comparison and scores for July-September are close to those of January-March. Error radius scores for these periods are, again, consistent with constant direction error. April-June produces the lowest error radius at day thirty. Distance regression slope and correlation are low throughout the comparisons of April-June and July-September indicating low correlation between predicted and observed displacement magnitudes during these months. April-June produces the lowest vector correlation scores, likely due to inaccurate displacement magnitude and angle predictions. Vector correlation is also low for July-September but higher than April-June because angles are predicted more accurately during this time.

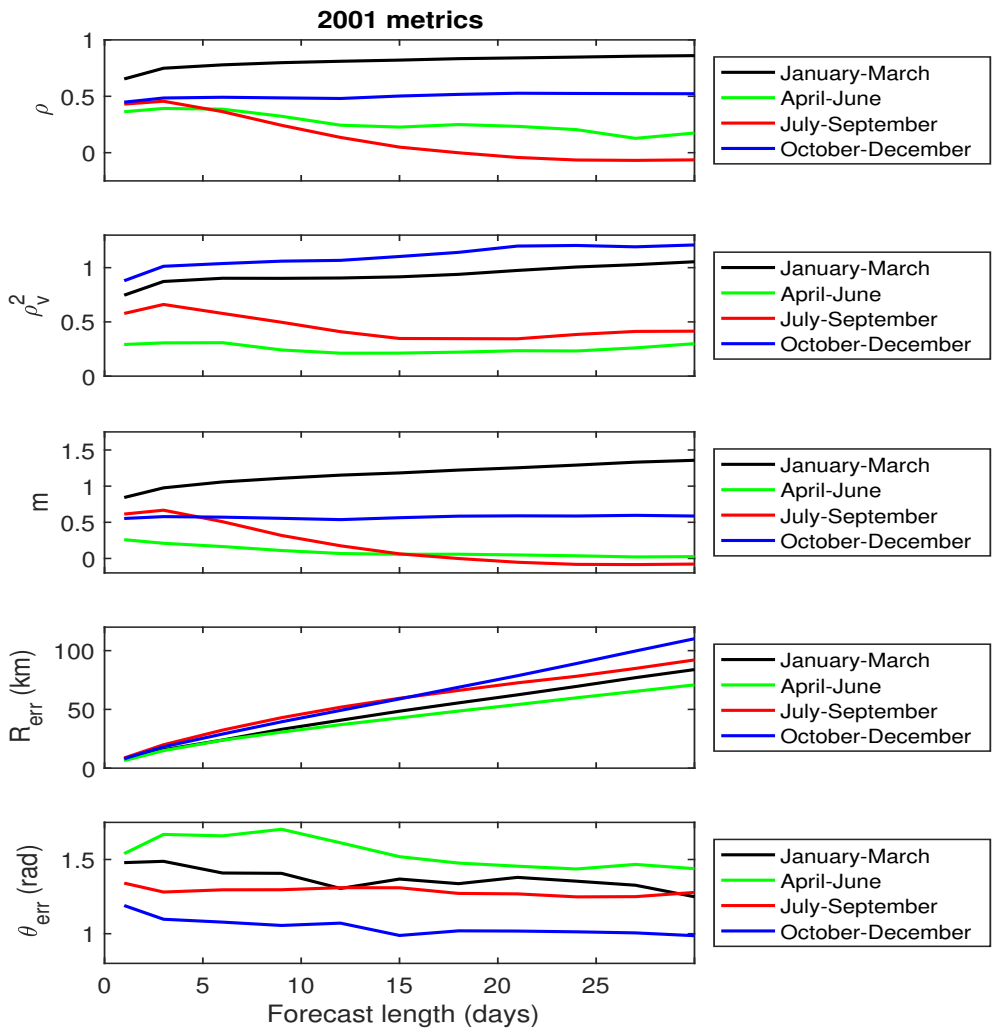

Figure 4.1: Distance correlation, vector correlation, regression slope, error radius, and direction error for the three-month comparisons of 2001. Scores are generally better for January-March and October-December, with the exception of error radius and direction error scores.

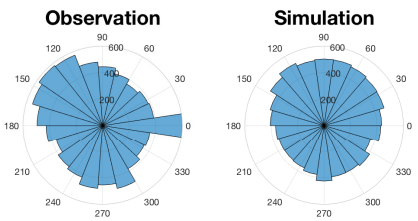

(a) 1-day forecast

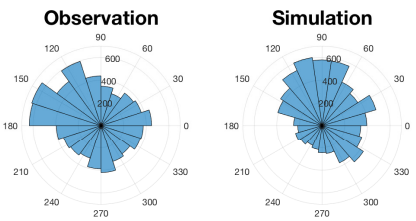

(b) 15-day forecast

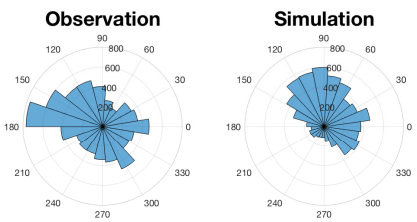

(c) 30-day forecast

Figure 4.2: Histograms for all 2001 observation and simulation displacement angles. The distributions become more dissimilar as the forecast length increases.

Figure 4.2 shows the distributions of all 1-day, 15-day, and 30-day forecast observation and simulation displacement angles for 2001. At a forecast length of 1-day small displacement angles are under-predicted by the simulation. The frequency of directions is well matched for shorter forecast lengths compared to longer ones. However, this may be an artifact of comparing the full year as opposed to shorter time frames. Observations appear rotated 50° counterclockwise from simulations which is consistent with the approximate average of the 1-day forecast direction error of Figure 4.1 (close to 60°).

Figure 4.3 shows the distributions of all observations and simulations for 1-day,

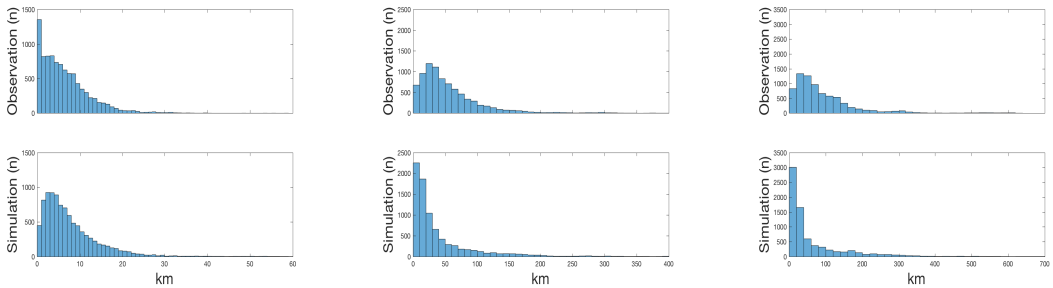

(a) 1-day forecast (b) 15-day forecast (c) 30-day forecast

Figure 4.3: Histograms for all 2001 observation and simulation displacement magnitudes, where n is the number of observations. The plots show over-prediction of small displacements for longer forecast lengths. Note, the y-axis scale differs between subfigures.

15-day, and 30-day forecast displacement magnitudes for 2001. Simulation outliers are excluded in the creation of the histograms. The largest displacement magnitudes predicted by the simulation for 1-day, 15-day, and 30-day forecasts are 72 km, 616 km, and 955 km, respectively. The plots show that displacements less than 1 km are under-predicted for shorter forecast lengths, while displacements smaller than 20 km are over-predicted for longer forecast lengths. In general, the distributions suggest magnitudes are being under predicted.

Figure 4.4 shows scatter plots of observation and simulation 1-day displacement magnitudes for January-March, along with the linear regression line and correlation coefficient. Even though the 1-day forecast plots show relatively good results in terms of distance correlation and regression slope, the scatter plot does not necessarily reflect this. In contrast the 30-day forecast plot clearly shows two different trends: one in which the model over-predicts smaller displacements (50 km and lower) and another which over-predicts larger displacements (400 km and higher). These two extremes likely compensate each other in the calculation of the linear regression and correlation coefficients. Thus, the scatter plots provide insight that cannot be captured solely using the metrics in Fig. 4.1.

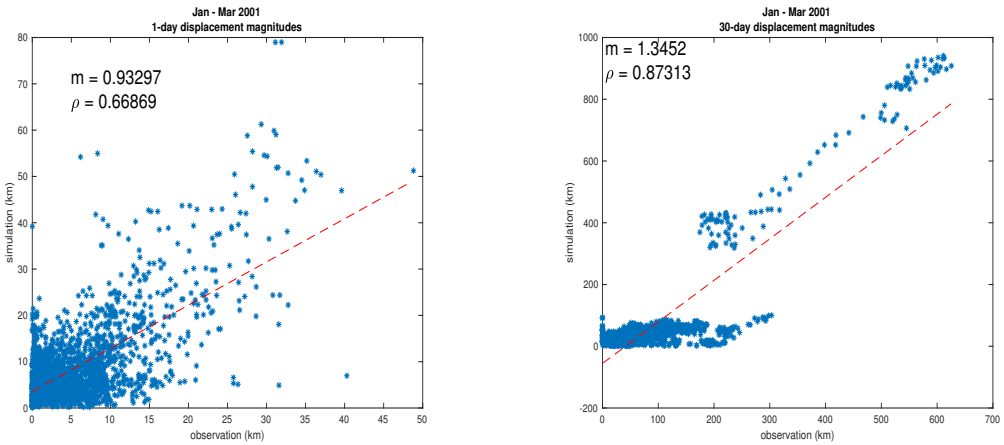

(a) 1-day displacements

(b) 30-day displacements

Figure 4.4: Scatter plots of observation (x-axis) and simulation (y-axis) displacement magnitudes for January-March, 2001. The plots show much scatter around the regression line in (a), and the influence of large displacements in the longer forecast length of (b).

Figure 4.5 shows the displacement statistic differences for displacement magnitudes for the three-month comparisons of 2001. July-September shows the best scores for all measures. This might be misleading considering the results shown in Figure 4.1 and the simulation may be consistently under-predicting displacement magnitudes. January-March and April-June show statistics are diverging with increasing forecast length, indicating the simulation might be more trustworthy over shorter time periods. Such a result has previously been observed in [9].

Figure 4.6 shows the statistic differences for displacement angles for the three month comparisons of 2001. The difference in mean angles shows January-March and October-December trended similarly and both of these periods scored similarly for vector correlation in Figure 4.1. The difference in mean angles increases for July-September contrary to the other periods examined. The difference in displacement angle standard deviations as well as variances increase with increasing forecast length, though January-March stayed close to observation.

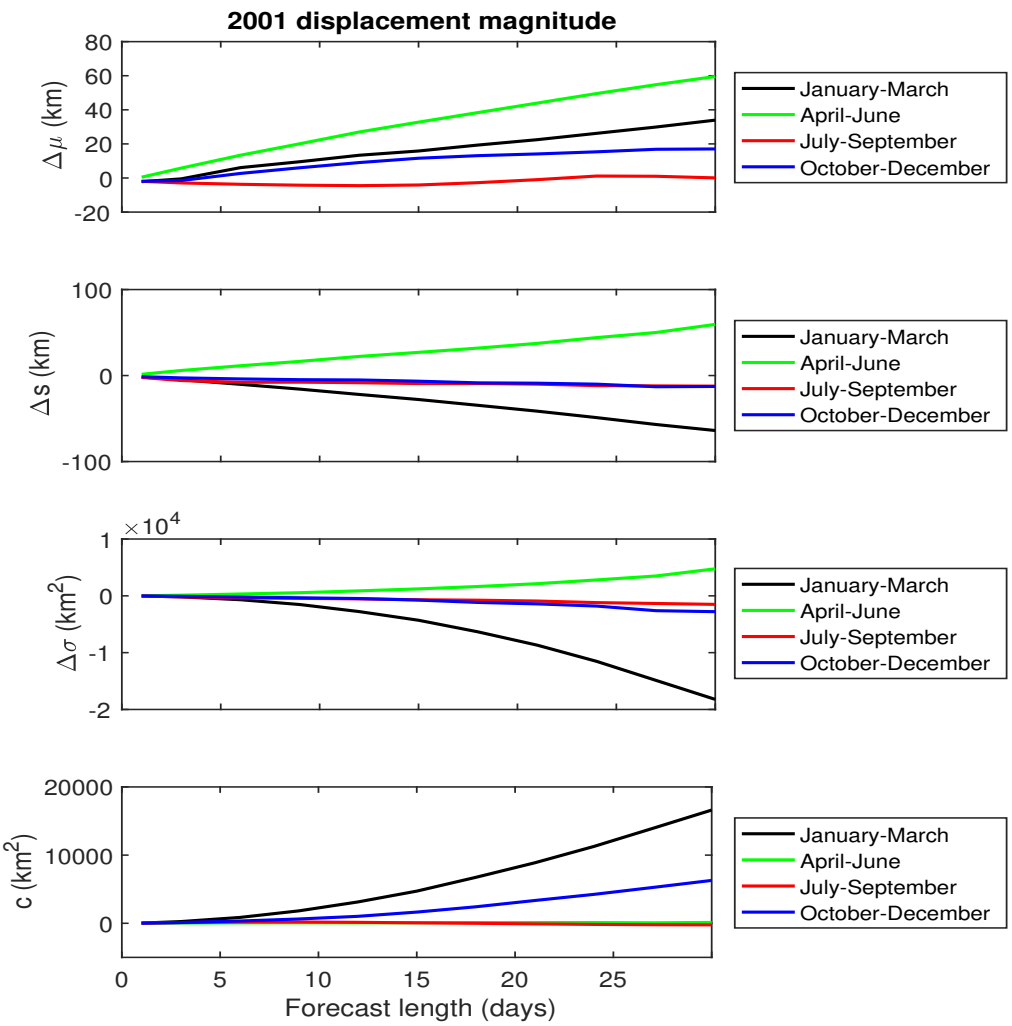

Figure 4.5: Difference of means, standard deviations, variances, and covariance of buoy and simulation point displacement magnitudes for all three-month comparisons of 2001. July-September and October-December have magnitude values closer to what is observed than other comparison months.

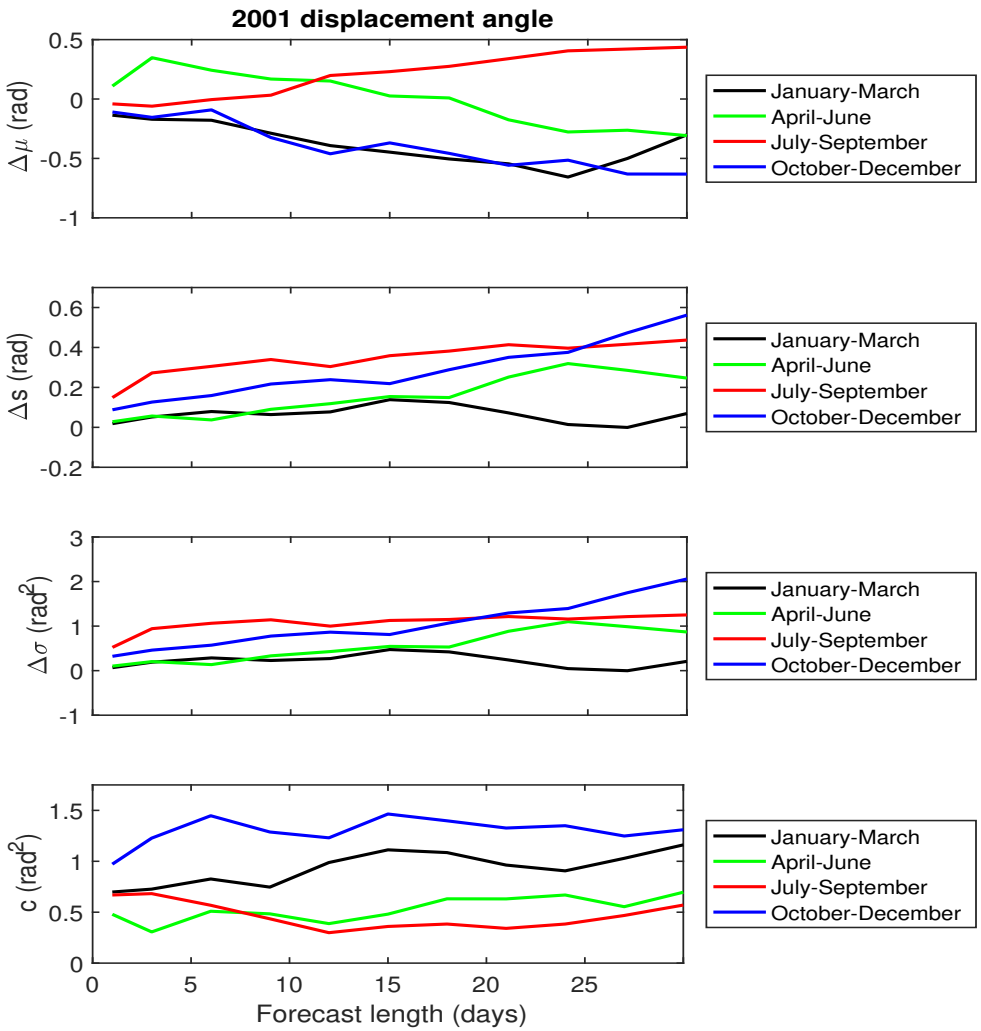

Figure 4.6: Difference of means, standard deviations, variances, and covariance of buoy and simulation point displacement angles for all three-month comparisons of 2001. The difference of average angles for January-March and October-December show similar trends. In terms of the range of displacement angles January-March and April-June are closest to what is observed.

The previous plots show that angle and magnitude errors in the simulation are persistent and contribute to error radius scores seen in the comparison. Average simulation displacement magnitude is too small apart from July-September. The variance in simulation magnitudes is too large for January-March as indicated by the regression slope and distance correlation scores for this period. There appears to be a similar trend in the difference of mean displacement angles apart from July-September.

2001 observation counts				
Forecast (days)	January - March	April - June	July - September	October - December
1	2193	2386	2364	2384
3	2068	2218	2182	2207
6	1996	2085	2048	2110
9	1914	1997	1925	2039
12	1829	1898	1825	1928
15	1765	1793	1721	1830
18	1678	1714	1630	1742
21	1620	1626	1541	1674
24	1544	1540	1412	1582
27	1464	1452	1328	1506
30	1381	1362	1266	1426

Table 4.1: Number of observations from buoys used to produce the metric scores for the three month comparisons of 2001. The number of observations available decreases with increasing forecast length.

Table 4.1 shows the number of buoy displacements for each forecast length used in the 2001 comparison with displacements of the simulation MPM_ice. Though the number of observations decreases with increasing forecast length, there are enough at day thirty to make a meaningful comparison.

4.2.2 2003

Figure 4.7 shows the metric scores for all comparisons made to buoys for 2003. January-March, in black, and October-December, in blue, produce near constant direction errors throughout the comparison which is consistent with linearly increasing error radii for these months. Distance regression slope for January-March peaked at day three and remains close to one-half through a twenty-five day forecast, while distance correlation increases throughout the comparison. Regression slope behaves similarly for October-December, though distance correlation remains low throughout the comparison, implying weak correlation between observed and simulated displacement magnitudes. Vector correlation scores are very similar for January-March which better predicts directions, and October-December which better predicts magnitude.

April-June, in green, gives the largest direction error through the duration of the comparison and corresponds to linearly increasing error radius with increasing forecast length. July-September, in red, had low direction error through day ten but is larger than all months besides April-June for the remainder of the comparison. Error radius for July-September increases linearly and produces the largest score at day thirty, suggesting issues with magnitude predictions during this time. Regression slope for April-June decreases throughout the comparison and corresponds to very low correlation coefficients, suggesting magnitudes are not predicted well during this time. Regression slope for July-September remains low, though higher than April-June, throughout the comparison and is associated with low, though again higher than April-June, correlation coefficient. Vector correlation is very low, and relatively constant, for April-June driven by bad direction and magnitude predictions. For July-September vector correlation scores are higher and closer to scores seen in January-March and October-December. This is most likely due to relatively better direction predictions for July-September as the maximum direction error score, at eighteen days, corresponds to the minimum vector correlation score.

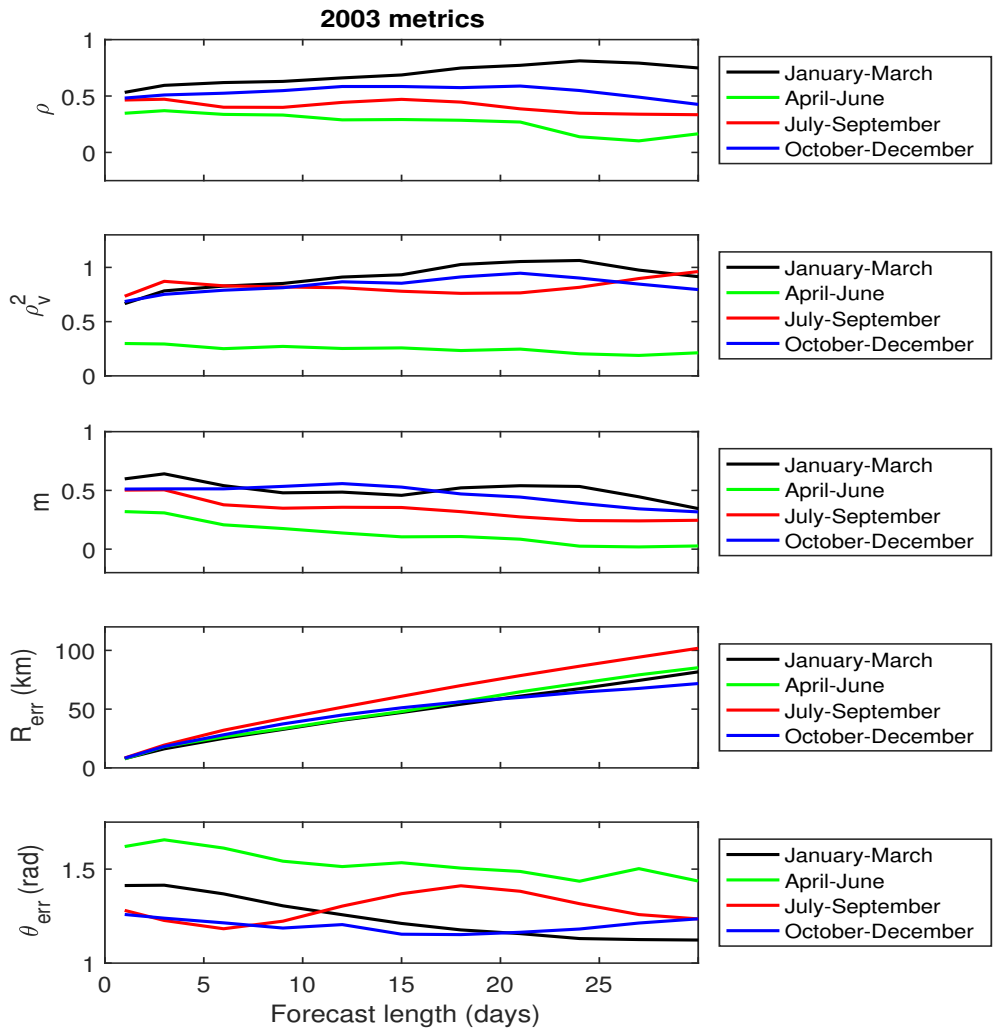

Figure 4.7: Distance correlation, vector correlation, regression slope, error radius, and direction error for all three-month comparisons of 2003. January-March and October-December score better than April-June and July-September for most forecast lengths. The comparison of April-June has the worst scores with the exception of error radius.

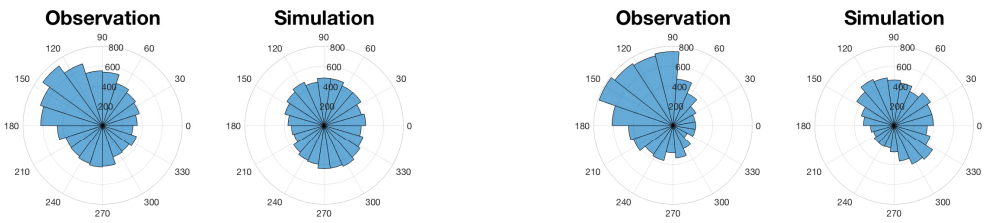

(a) 1-day forecast

(b) 15-day forecast

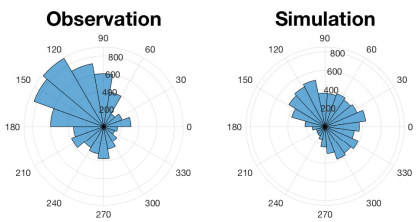

(c) 30-day forecast

Figure 4.8: Histograms for all 2003 observation and simulation displacement angles for 1-day, 15-day, and 30-day forecast displacements.

Figure 4.8 shows the distributions of all 1-day, 15-day, and 30-day forecast observation and simulation displacement angles for 2003. The plots show that the distributions of predicted displacements for short forecasts are close to those observed. While the distributions are similar, the predicted distribution of displacement angles appears to be more uniform than observations. These plots provide further evidence that there are issues with displacement angles in the simulations.

Figure 4.9 shows the distributions of all observation and simulation 1-day, 15-day, and 30-day forecast displacement magnitudes for 2003. The distribution of simulated 1-day forecast displacement magnitudes is similar to what is observed. However, for

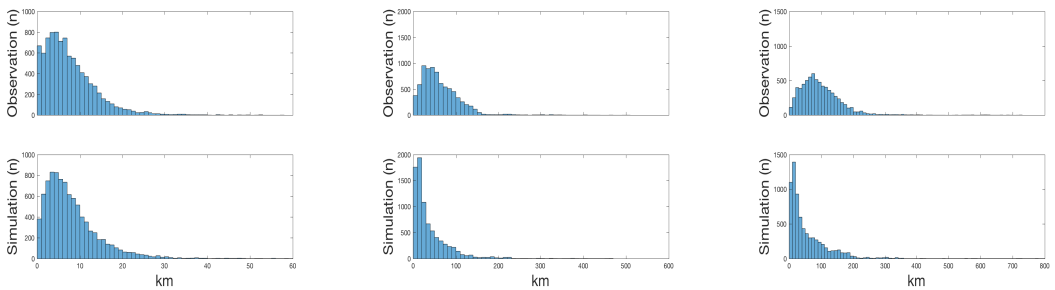

(a) 1-day forecast (b) 15-day forecast (c) 30-day forecast

Figure 4.9: Histograms for all 2003 observation and simulation displacement magnitudes for 1-day, 15-day, and 30-day forecast. The plots show over-prediction of small displacements for longer forecast lengths.

30-day forecasts the simulation over-predicts displacements smaller than 40 km and under-predicts displacements larger than 120 km. Similarly to 2001, the simulation under-predicts larger displacements for longer forecast lengths.

Figure 4.10 shows scatter plots of observation and simulation 1-day and 30-day forecast displacement magnitudes for January-March, along with the linear regression

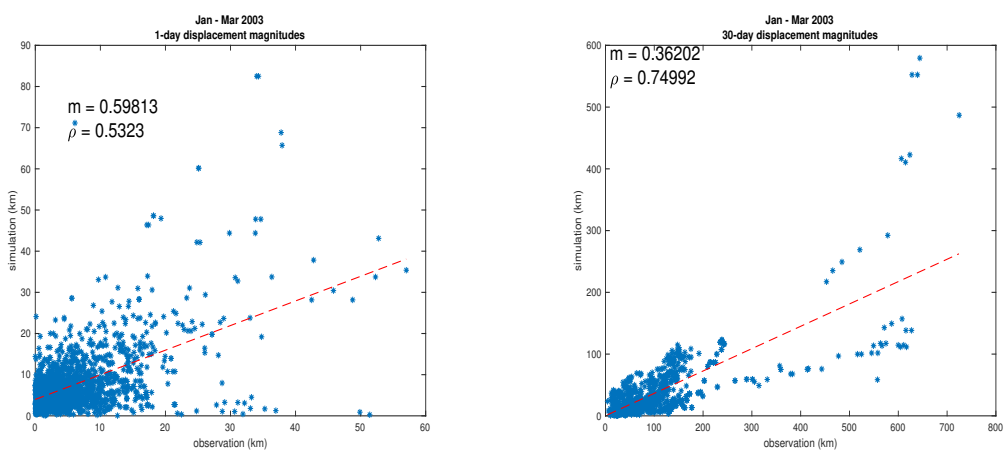

(a) 1-day forecast (b) 30-day forecast

Figure 4.10: Scatter plots of observation (x-axis) and simulation (y-axis) displacement magnitudes for January-March, 2003.

line and correlation coefficient. (The plots represent the most accurate displacement magnitude predictions from the 2003 comparison to buoys, according to the metrics shown in Figure 4.7.) Similarly to what is shown for 2001 in Figure 4.3, regression slope and correlation coefficient scores should be interpreted with care and in terms of one another.

Figure 4.11 shows the differences of statistics for simulation and buoy displacement magnitudes for all three-month comparisons for 2003. Averaged simulation magnitudes for all three-month comparisons are smaller than those observed. The large difference in variance shows the range of magnitudes predicted is too large far all three-month periods and more so for January-March. Contrary to what is observed in Figure 4.5, simulated displacements in 2003 are consistently under-predicting the range of displacement magnitudes.

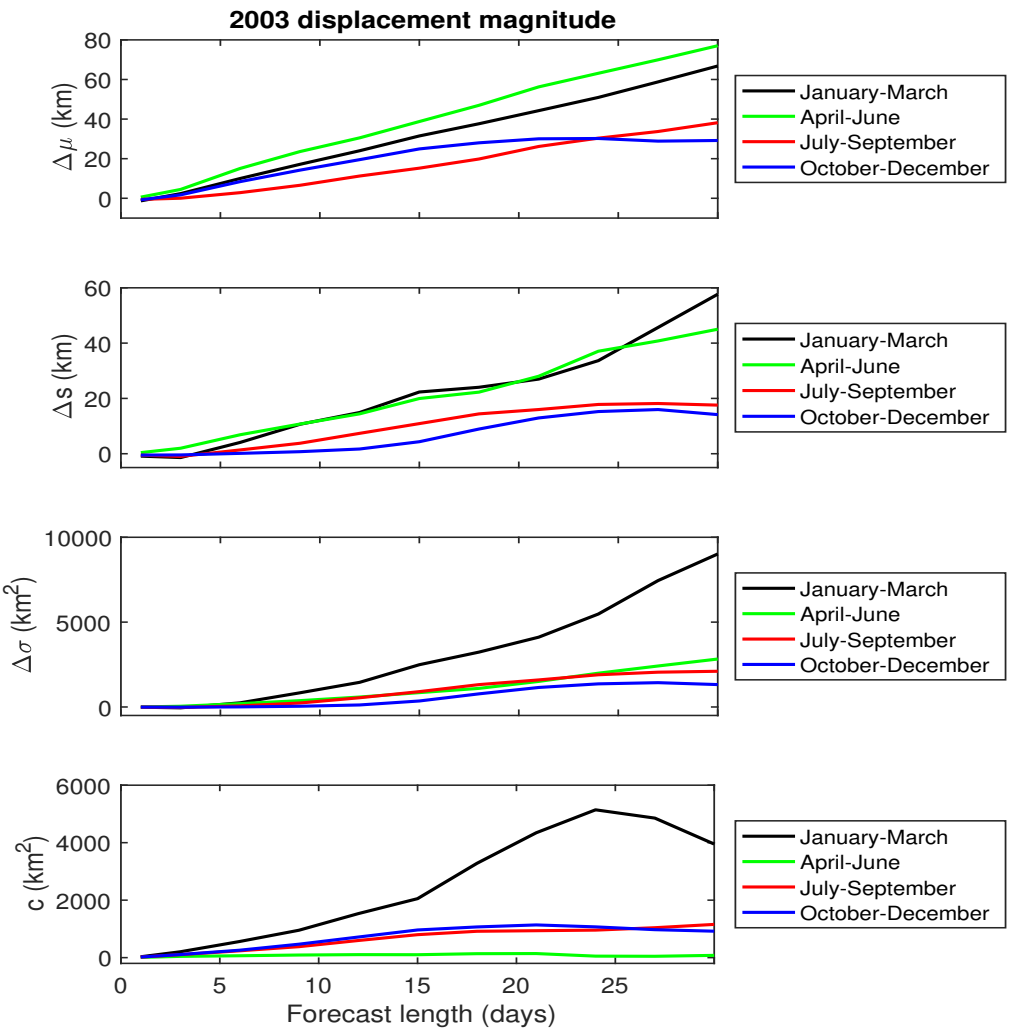

Figure 4.11: Difference of means, standard deviations, variances, and covariance of buoy and simulation point displacement magnitudes for all three-month comparisons of 2003. July-September and October-December produce displacement magnitudes closest to observation on average.

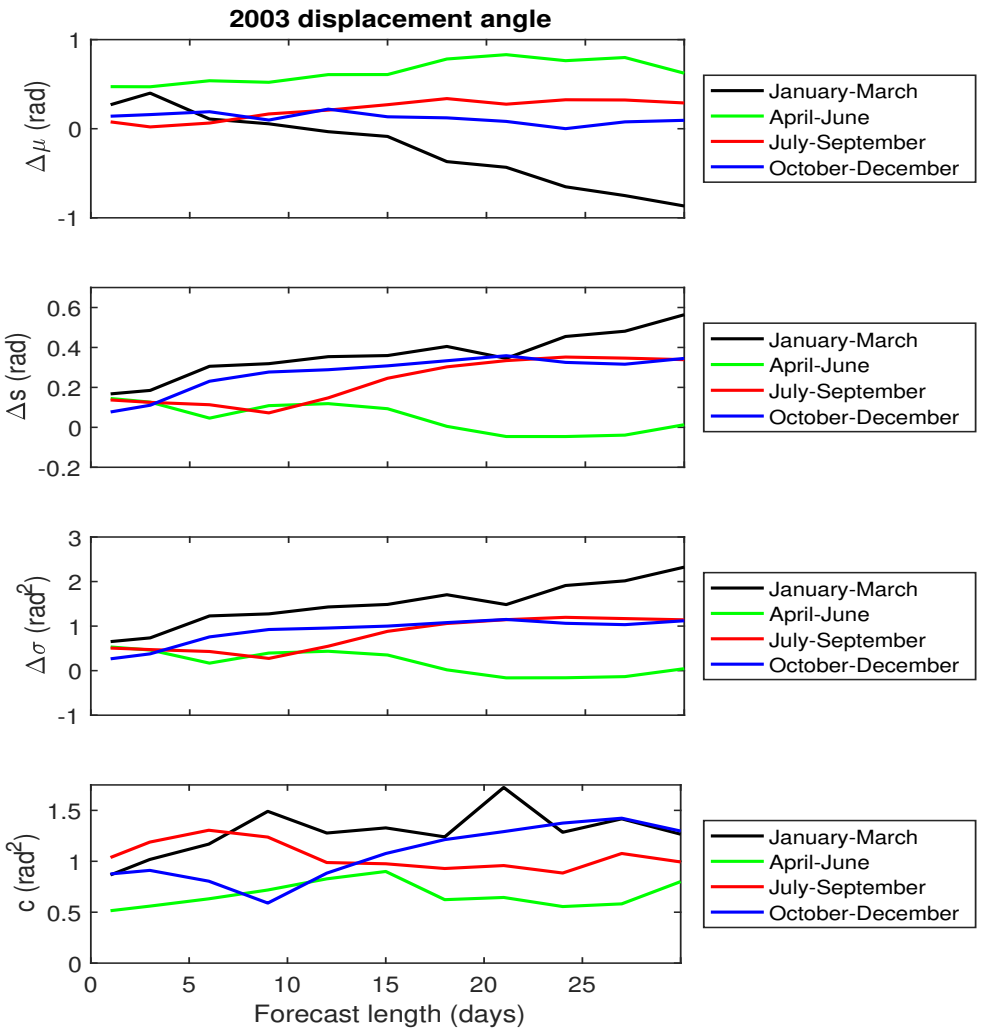

Figure 4.12: Difference of means, standard deviations, variances, and covariance of buoy and simulation point displacement angles for the three-month comparisons of 2003. The averaged simulation displacement angles for January-March are continuously decreasing with forecast length compared to observation. We do not see such a trend for the three other periods.

Figure 4.12 shows the difference of statistics for simulation and buoy displacement angles for all three-month comparisons for 2003. The average simulation displacement angles for January-March are continuously decreasing with respect to forecast length compared to observation. However, this trend is not apparent for any of the other three-month periods. Simulation for July-September shows the best statistical agreement compared to observations.

The results in Figure 4.7 are counter-intuitive when taking into account the statistics shown in Figure 4.12. For example, the direction error is decreasing with increasing forecast length while the difference in mean angles grows worse. This might suggest that the small values seen in the difference in means with increasing forecast length may be due to cancellation error. In contrast the direction error for October-December does not vary strongly with forecast length nor does its statistics.

2003 observation counts				
Forecast (days)	January - March	April - June	July - September	October - December
1	1530	2394	2392	2755
3	1464	2272	2262	2602
6	1398	2144	2120	2504
9	1342	2024	1996	2404
12	1273	1922	1877	2289
15	1209	1825	1767	2194
18	1159	1733	1646	2089
21	1106	1644	1539	1986
24	1050	1543	1442	1896
27	1001	1456	1348	1801
30	938	1369	1268	1699

Table 4.2: Number of observations used to produce the metric scores for three month comparisons of 2003. Observation data available for comparison decreases with increasing forecast length.

Table 4.2 shows the number of buoy displacements for each forecast length used in the comparison with displacements from the simulation MPM_ice. This table shows similar patterns as 2001 from which we can draw similar conclusions.

4.3 Comparison of averaged-RGPS and MPM_ice

In order to compare to averaged-RGPS, simulation displacements are interpolated to a grid each day and these daily displacements are averaged for the month. Due to

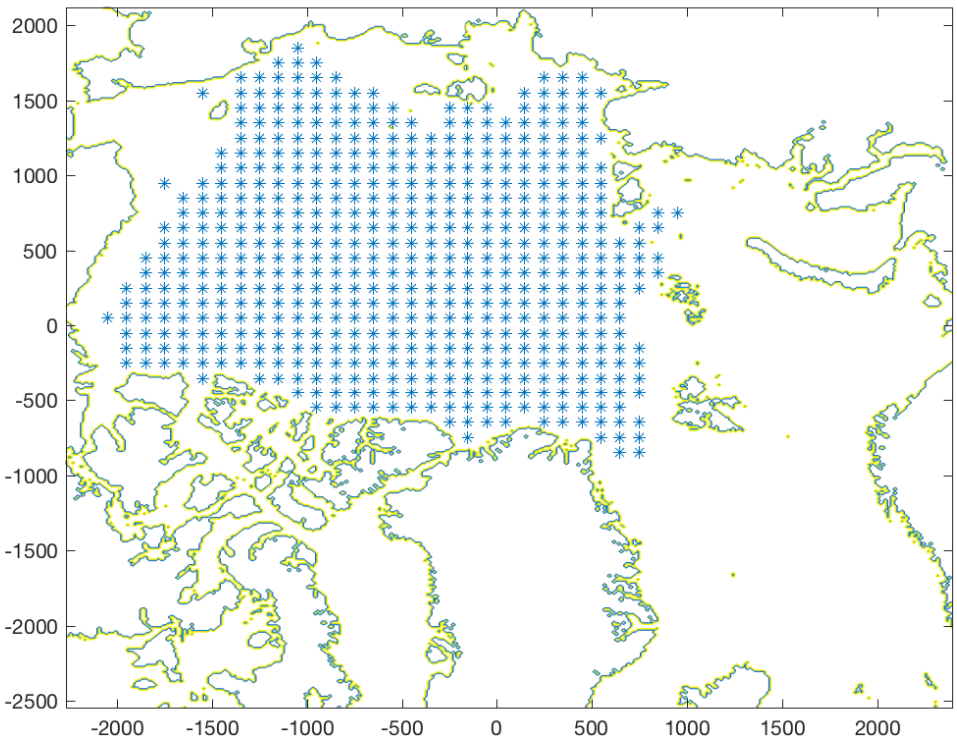

Figure 4.13: Region of RGPS comparison corresponding to ice minimum. This ensures a constant number of points (541) throughout the comparison.

the fact that observation and simulation do not always agree on the sea ice extent, we choose a fixed domain, shown in Figure 4.13. This region corresponds to the observed sea ice minimum extent which ensures a constant number of points (541) throughout the comparison. This domain is chosen in order to give a consistent picture of ice displacements throughout the year. Without this choice of domain, the

number of observation points would change in time, complicating interpretation of the metrics. Moreover, if the simulation and observation do not agree on ice extent, then there would be points with nonzero observations and missing simulations, or vice versa. At present it is not clear how to treat the missing values.

4.3.1 2001

Figure 4.14 shows the metric scores for the comparison of daily-averaged displacements for each month of 2001. Direction error scores, with the exception of March, are lower for winter months. Error radius scores are low with the exception of September through November. The fact that direction error scores are low during this time suggests that errors in magnitude are responsible for low error radius scores. Regression slope and distance correlation also show better scores for winter months, however in September regression slope shows a spike above one suggesting predicted magnitudes are too large. This fact agrees with the error radius and direction error scores. Vector correlation, consistent with the rest of the metrics, shows better scores for winter months.

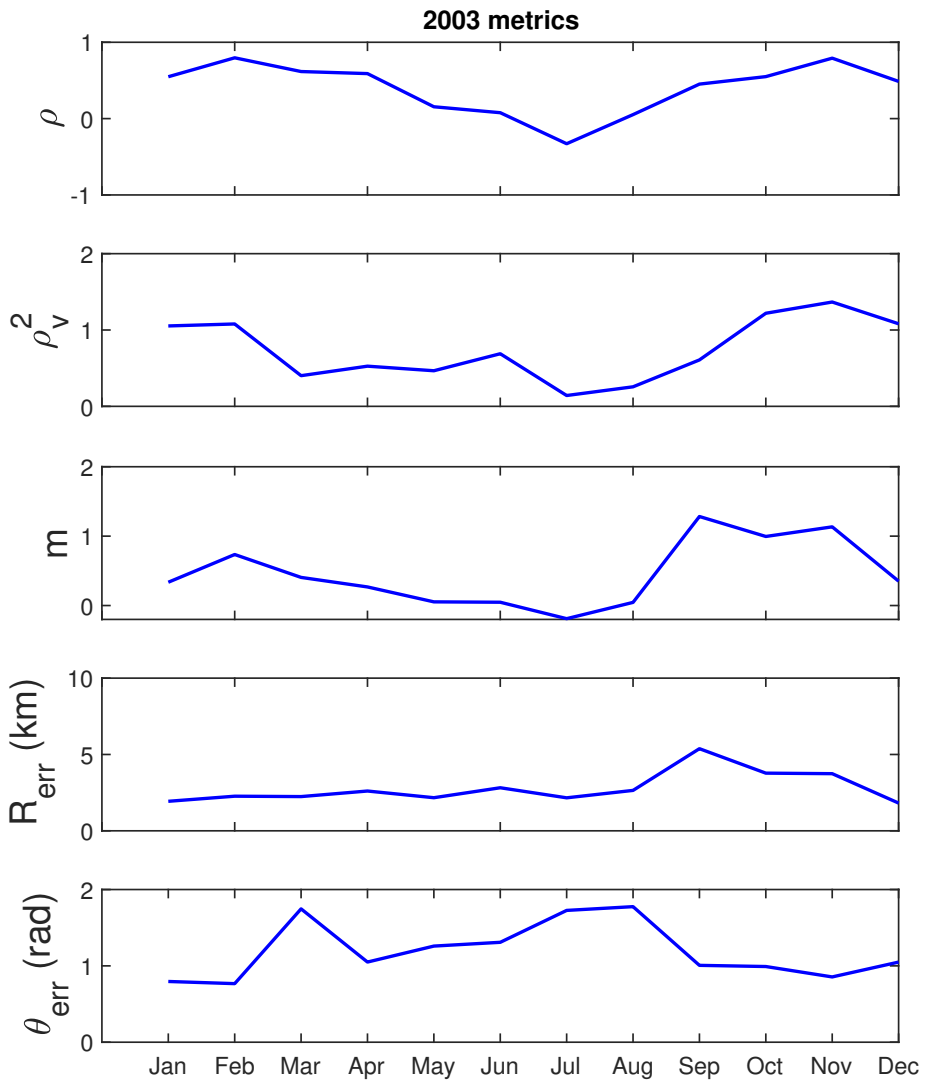

Figure 4.14: Distance correlation, vector correlation, regression slope, error radius, and direction error for daily-averaged displacements for each month of 2001. Scores are generally better for winter months.

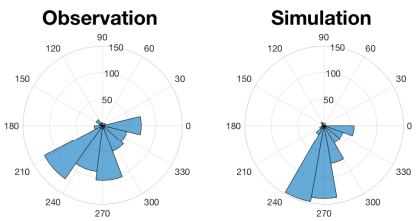

(a) January

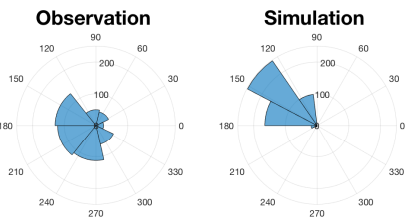

(b) March

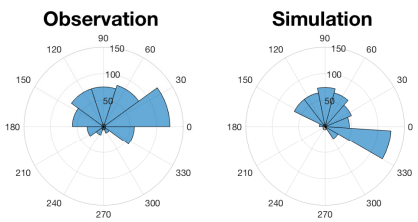

(c) September

Figure 4.15: Histograms for 2001 observation and simulation displacement angles. The plots show under-prediction of the range of displacement angles by the simulation.

Figure 4.15 shows the distributions of observation and simulation displacement angles for January, March, and September. The plots show that the ranges of displacement angles predicted are too small for these months and the highest frequency of simulated direction angles never match those of the observations.

Figure 4.16 shows the distributions of observation and simulation displacement magnitudes for January, March, and September. The plots show the model does not accurately predict the distribution of simulated displacement magnitudes. January and March under-predict larger displacements and over-predict smaller dis-

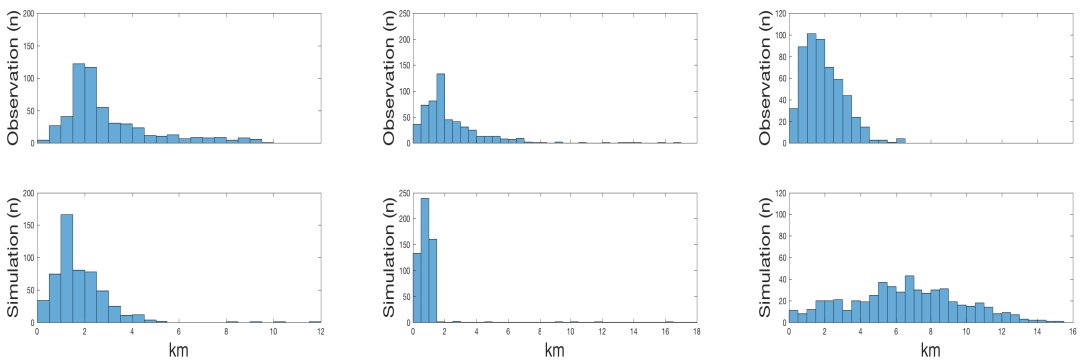

(a) January (b) March (c) September

Figure 4.16: Histograms for January, March, and September, 2001 observation and simulation displacement magnitudes. Issues in September are apparent, while January and March show under-prediction of larger displacements.

placements. These results are consistent with the small regression slopes seen for these months. September shows over-prediction of large displacements which helps to explain the large regression slope seen in the comparison.

Figure 4.17 plots observation and simulation displacement magnitudes for March and September 2001. The scatter plot for March emphasizes that simulated displacements over 2 km are not colocated with observed displacements of similar magnitude, which is consistent with the distribution in 4.16 (b). Although September has an improved regression slope, the scatter in the data do not show a strong linear relationship evidenced by the relatively low correlation coefficient.

Figure 4.18 (a) shows the means, standard deviations, variances, and covariance of simulation and averaged-RGPS displacement magnitudes. Mean displacement magnitude as well as the range of displacement magnitudes are too small through August and too large for September through November. This is consistent with the interpretation of the regression slope and distance correlation scores made from Figure 4.14.

Figure 4.18 (b) shows the means, standard deviations, variances, and covariance of averaged simulation and averaged-RGPS displacement angles. Predicted mean displacement angles for March and November are far from observation compared to all other months. The average angle predicted for June is close to observation and so is its variance. However, the direction error for June in Figure 4.14 suggests these relatively good results may be due to cancellation.

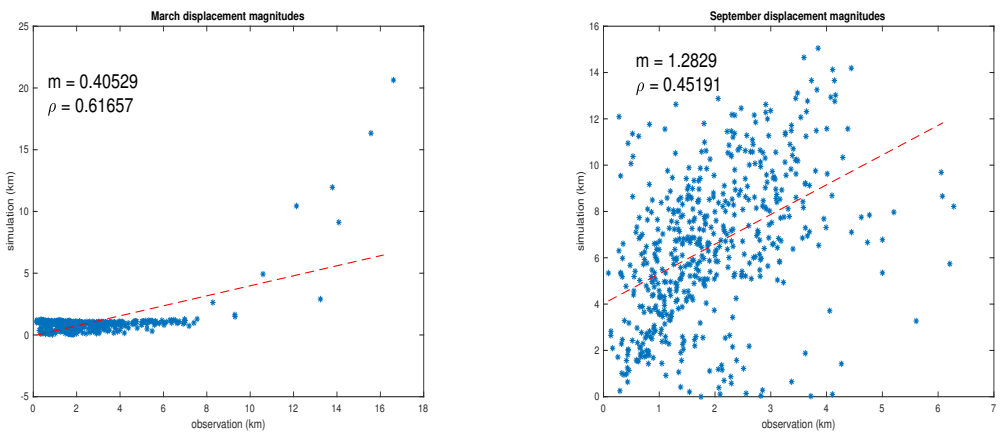

(a) March (b) September

Figure 4.17: Scatter plots of observation (x-axis) and simulation (y-axis) displacement magnitudes for March and September, 2001. The scatter plot for March emphasizes that simulated displacements up to 8 km do not necessarily align well with observed displacements of similar magnitude, hence the low regression slope. The scatter plot for September shows an improved regression slope though lower correlation.

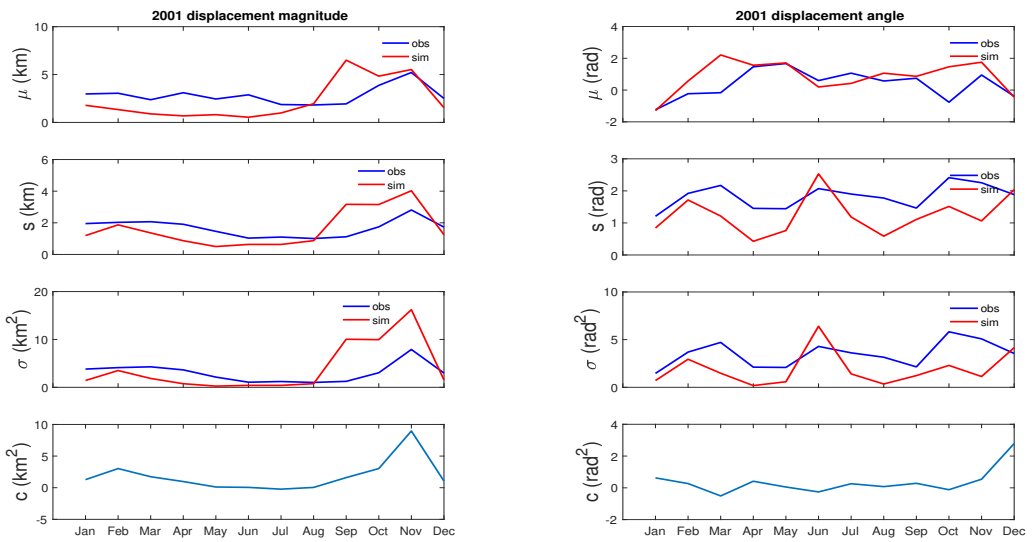

(a) Magnitude (b) Angle

Figure 4.18: Observation (blue) and simulation (red) averaged magnitude and angle statistics for 2001. The plots show that mean displacement is under-predicted through August. The variance of predicted displacement angles is too small apart from June.

4.3.2 2003

Figure 4.19 shows the scores for daily-averaged displacements for each month of 2003. Apart from February and March direction error scores are close to or greater than one. Similarly to the 2001 comparison in Figure 4.14, scores are higher for winter months. Trends in the error radius scores are less apparent, though the lowest scores are obtained in February and November. Vector correlation, distance regression slope, and distance correlation scores trend similarly and show worse scores for summer months, though there is an improvement in scores for August.

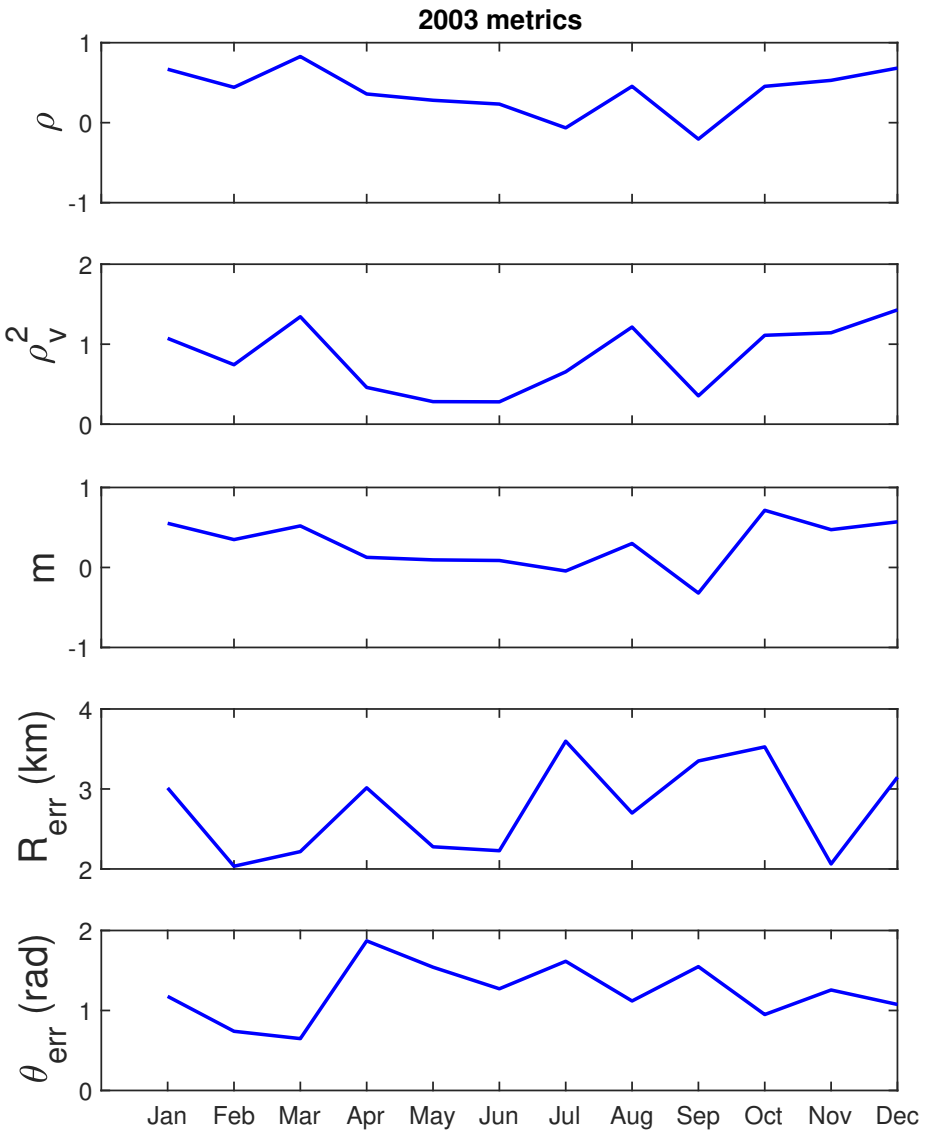

Figure 4.19: Distance correlation, vector correlation, regression slope, error radius, and direction error for daily-averaged simulation displacements for 2003. Scores are generally better for winter months, though less apparent as in 2001. September scored among the worst for all metrics.

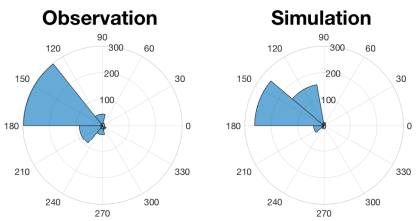

(a) March

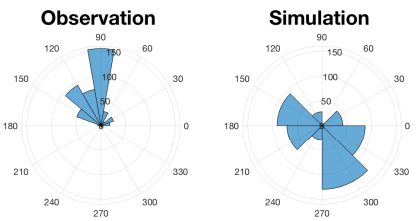

(b) April

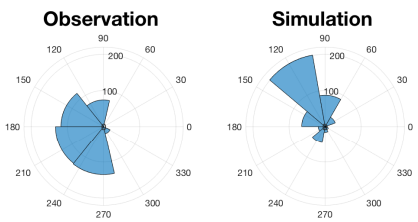

(c) September

Figure 4.20: Histograms for 2003 observation and simulation displacement angles. Apart from March the range of displacement angles predicted is too small. The average angles predicted for April and September are far from observation.

Figure 4.20 shows the distributions of observation and simulation displacement angles for March, April, and September 2003. (Note: April was examined instead of January due to the striking difference in direction error scores between March and April.) The distributions for March are very close which is consistent with the score for direction error in Figure 4.19, which is among the best. For April, which produced the highest direction error score, the distributions are very dissimilar, both in average direction and the variance of the distributions. September produced distributions closer to those seen in the comparison of 2001 in that the predicted range of displacement angles is too small and the means are rotated.

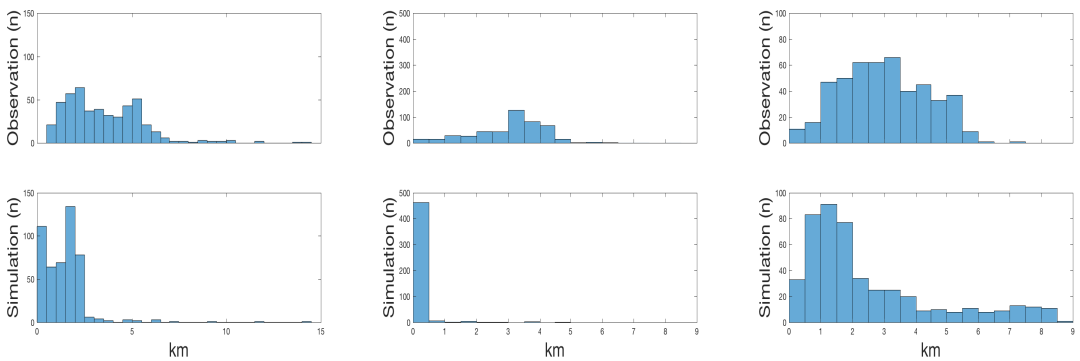

(a) March (b) April (c) September

Figure 4.21: Histograms for March, April, and September, 2003 observation and simulation displacement magnitudes. The plots show that small and large displacement are over- and under-predicted respectively by the simulation.

Figure 4.21 shows the distributions of observation and displacement magnitudes for March, April, and September. The distributions for March and April show over-prediction of displacement less than 1-2 km and under-prediction of displacement greater than 2 km. September shows over-prediction of displacements less than 1 km and greater than 6 km which helps to explain the very low regression slope and distance correlation scores in the comparison.

Figure 4.22 shows scatter plots of observation and simulation displacement magnitudes for March and September, the months that produce the best and worst regression slope and distance correlation scores, respectively. In March, there is a reasonable correlation between observed and simulated displacement magnitudes which is confirmed by the scatter plot. The regression slope is smaller than one, indicating that simulated displacements are too small. We also see this trend in the distribution of displacements shown in Figure 4.21. The scatter plot shows there is no meaningful relationship between observed and simulated displacement magnitude in September.

Figure 4.23 (a) shows the means, standard deviations, variances, and covariance

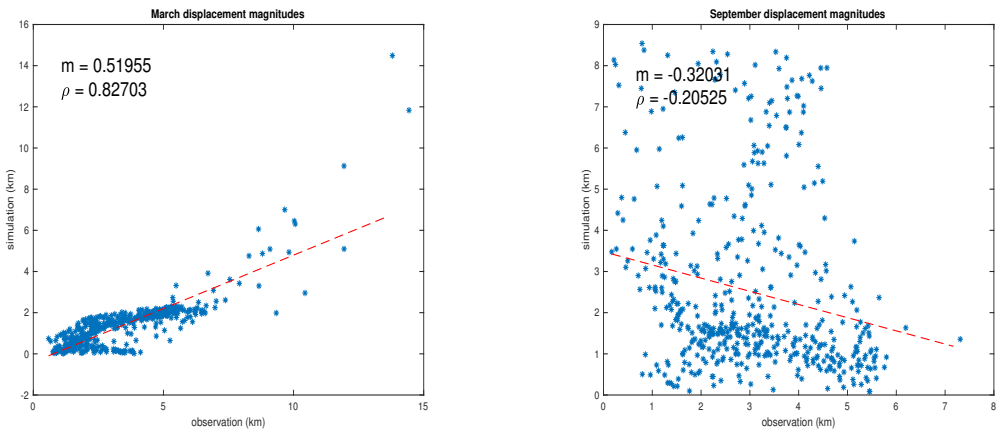

(a) March (b) September

Figure 4.22: Scatter plots of observation (x-axis) and simulation (y-axis) displacement magnitudes for March and September, 2003. Displacements for March show a good fit which is reflected in the high correlation coefficient, however the regression slope is too small. September gives a negative slope and the low correlation suggests this relationship is not meaningful.

of simulation and RGPS daily-averaged displacement magnitudes. Average displacement magnitudes predicted are too small for the full year with the exception of October. The variance of predicted displacement magnitudes is too small apart from September and October. The largest difference in mean displacement magnitudes is seen between February and June. Figure 4.19 shows that the error radius score is the smallest throughout these months indicating a consistent agreement between simulation and observation.

Figure 4.23 (b) shows the means, standard deviations, variances, and covariance for averaged simulation and RGPS displacement angles. Predicted mean displacement angles show wide variation across the year, though trends are similar to observation for January through March and October through December. With the exception of April the variance of predicted displacement angles is too small. The worst direction error scores occur in April, July, and September and these months

also correspond to the largest difference in mean displacement angles.

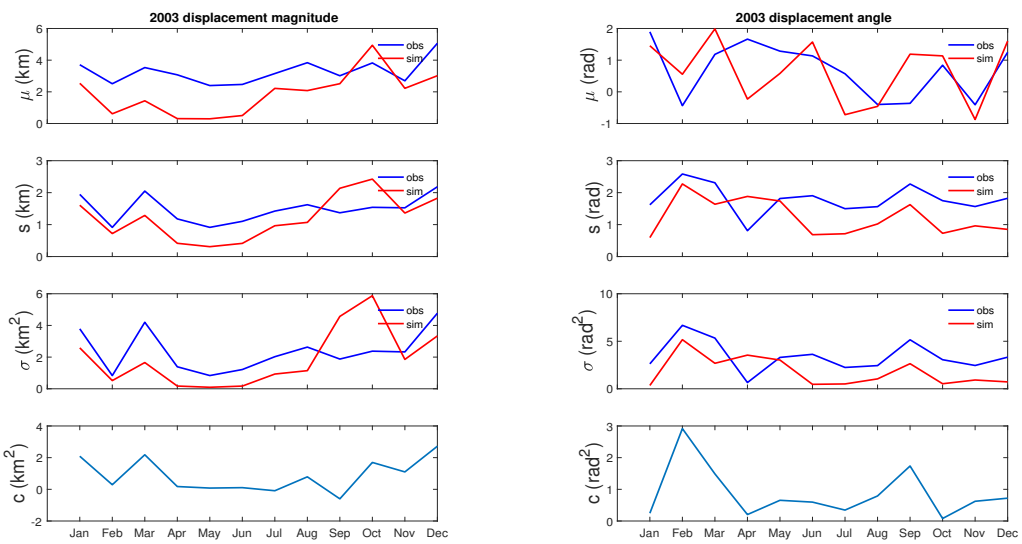

(a) 2003 displacement magnitudes.

(b) 2003 displacement angles.

Figure 4.23: Means, standard deviations, variances, and covariance between daily-averaged RGPS and simulation displacement magnitudes (panel (a)) and angles (panel (b)) for 2003. Mean displacement magnitudes predicted are too small apart from October. Average displacement angles predicted for April are far from observation.

4.4 Wind turning angle investigation

As wind speeds are generally measured at altitude, a wind turning angle parameter exists in the simulation to account for the Ekman spiral which causes wind velocities closer to the surface to rotate relative to the direction of motion at altitude. In Sections 4.3 and 4.4 the wind turning angle was set to 0.5 radians in the simulation which was found to be incorrect. In order to determine whether this parameter is responsible for the systematic direction errors observed in the comparisons, we reran the 2001 simulation with two different wind turning angles: -0.5, and 0 radians. In this section we denote Δ as the difference in metric scores using a new wind turning angle with respect to 0.5 rad. For example, $\Delta\rho = \rho_0 - \rho_{0.5}$ where ρ_0 and $\rho_{0.5}$ are the scores for distance correlation with 0 and 0.5 wind turning angles, respectively.

4.4.1 Buoy comparison

Figure 4.24 shows the difference in metric scores comparing the results between simulations using -0.5 rad and 0.5 rad wind turning angle. Direction error gets worse in October-December for forecast lengths of one and sixteen days but shows improvement otherwise. Error radius remains somewhat unchanged for April-June and July-September but improves for the two other periods. Other than October-December distance correlation and vector correlation are improved with a wind turning angle of -0.5 rad. Regression slope improves for January-March at day thirty but October-December becomes worse.

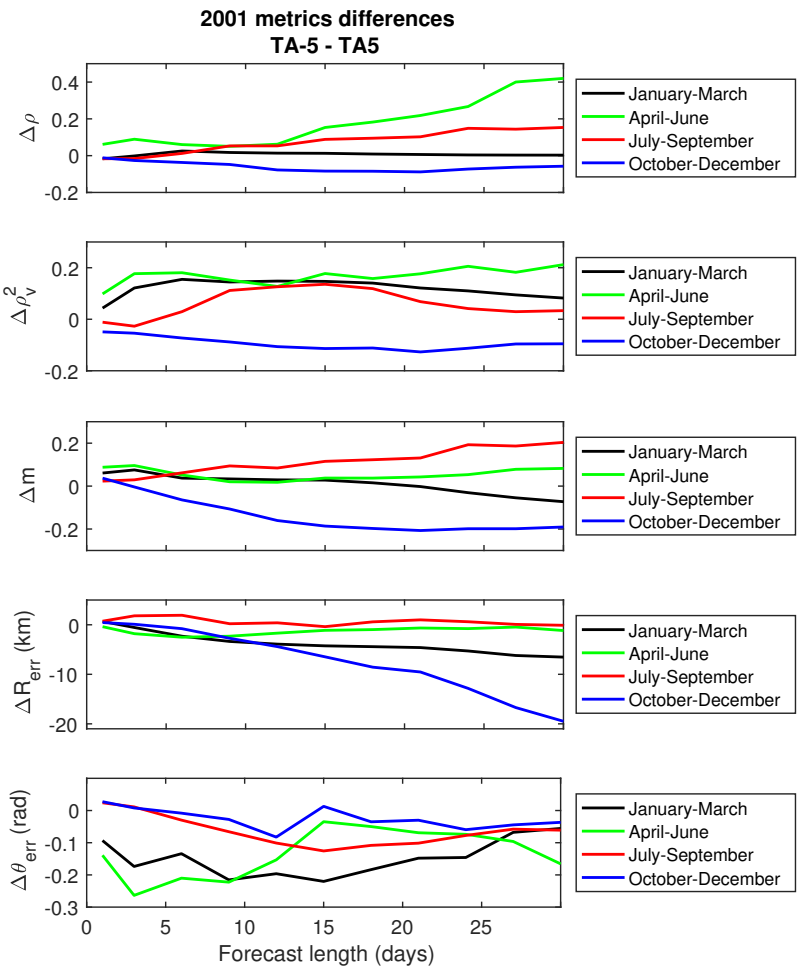

Figure 4.24: Metric scores with wind turning angle 0.5 rad subtracted from scores with wind turning angle -0.5 rad. Direction error, error radius, and vector correlation scores show some significant improvements when using a wind turning angle of -0.5 rad. The three other scores improve for each period besides October-December.

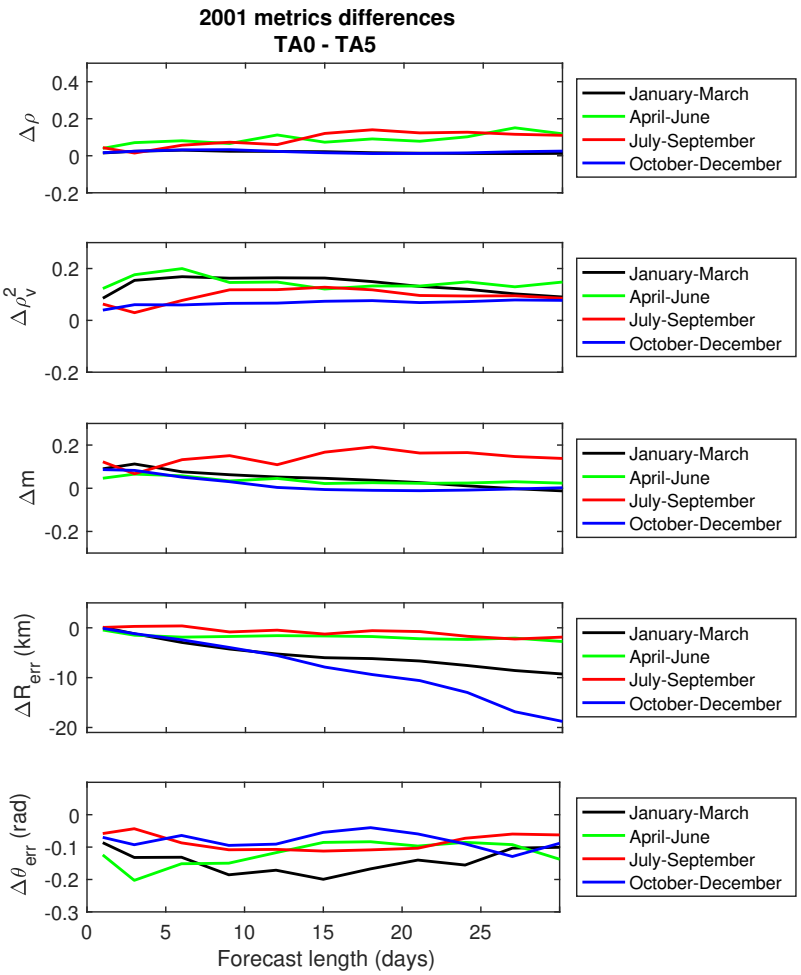

Figure 4.25: Metric scores with wind turning angle 0.5 radians subtracted from scores with wind turning angle 0 rad. Scores show more consistent improvements, though smaller in magnitude than with -0.5 rad.

Figure 4.25 shows the metric scores for the comparison of 2001 with wind turning angle 0.5 rad, subtracted from the scores with 0 rad. Direction error and error radius scores decrease showing an improvement for these metrics with 0 rad wind turning angle. Distance correlation and vector correlation scores are non-negative showing that scores improve or are unchanged for these metrics. Switching the turning angle to either 0 or -0.5 improves the metric scores and, in general, the improvements are comparable between the two different wind turning angles.

4.4.2 RGPS comparison

Figure 4.26 shows the metric scores for the RGPS comparison of 2001 with wind turning angle 0.5 rad subtracted from the scores with -0.5 rad in red, and 0 rad in black. Direction error improves for March, April, and November with wind turning angle -0.5 rad, but gets worse in January, June, October, and December. For wind turning angle 0 rad, direction error shows small improvements or no change throughout the year. Error radius scores are similar for both wind turning angles, though -0.5 rad shows improvement of greater magnitude in November. Regression slope scores also trend similarly for both wind turning angles. Distance correlation shows more consistent improvement for wind turning angle of 0 rad. While a -0.5 rad wind turning angle shows improvements of greater magnitude in April and May its scores are worse in March and October. Vector correlation scores were very similar apart from April.

The results for the wind turning angle comparisons with buoys and RGPS are similar. While 0 rad wind turning angle produces more consistent, though smaller, improvements, -0.5 rad produces improvements of greater magnitude overall. It is apparent, however, that both new wind turning angles show improvements over the original wind turning angle.

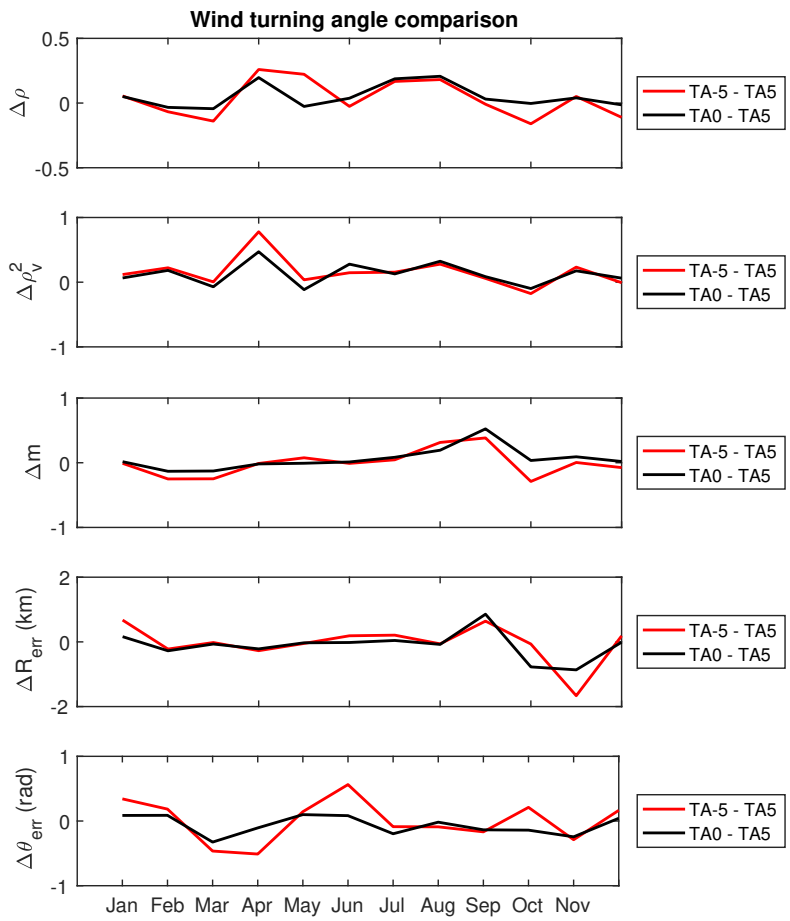

Figure 4.26: Metric scores for the RGPS comparison of 2001 with wind turning angle 0.5 rad subtracted from the scores with wind turning angle of -0.5 rad (red) and 0 rad (black). Similarly to the comparison with buoys, wind turning angle of 0 rad shows consistent improvement, while -0.5 rad produces some improvements, but of greater magnitude.

Chapter 5

Discussion

The averaged-RGPS data set presents several challenges with respect to the way zero displacements should be handled. The metrics are sensitive to the number of points being considered and many zero displacements can significantly affect scores and misguide their interpretation. In the comparison we restrict the domain to ensure that ice is present for the full year to prevent the number of observations and zero displacements from affecting the analysis. However, this restricted region excludes areas where ice is being exported from the Arctic Ocean, and therefore will not provide any information as to how well the simulation is performing in these regions.

The metrics defined in Chapter 2 are used to compare two-dimensional vectors, particularly displacements. In the comparison, zero displacement was assigned if a simulation point melted when it was not predicted to. This however may not be appropriate, as the metrics were chosen for their ability to take into account both magnitude and direction quantities. It may be unsuitable to have these particular metrics examine zero predicted displacement where displacements were observed, though this behavior should be penalized in model validation. If zeros are allowed for comparison, and if the domain of the comparison is increased to include more

ocean and therefore more ice-free surface area, then the model will perform better by predicting no ice in these regions but the simulation will not have improved in what it was designed to do. This bias is currently poorly understood and requires further investigation.

The interpretation of the regression slope and distance correlation also presents a challenge. We show using scatter plots that, even when good scores are assigned, the data may not represent a good fit. It might be that the observation and simulation magnitude data are not, in fact, linearly related in which case these metrics will be less useful. Since the scatter plots show a clustering of points near zero, it might be useful in the future to analyze a log-transform of the data, as this may give a clearer picture of how smaller observed and simulated displacements are related.

In the comparison with buoys a single MP with the shortest straight line distance to a buoy is found and tracked for the forecast period. However, the ice cover motion is discontinuous and it is possible that a buoy and MP could start on opposite sides of a fracture and drift apart. Thus, a MP starting slightly further from the buoy, but on the same side of the fracture, might track the buoy displacement more faithfully. In the future we plan to examine MPs in a neighborhood of each buoy to avoid this situation.

The results of Chapter 4 show that the simulation does not perform well in summer. During this period the ice cover is at a minimum and ice motion is governed for the most part by free drift. That the metric scores are low during the summer shows that the model may not capture this behavior well. However, observation error is also higher during this period. During fall and winter the simulation performs better according to the metrics, especially the period from October to December when ice is refreezing. The performance of the simulation from January through March is better than summer but worse than from October to December. At the start of the year, the simulation initializes the ice as solid and unfractured which may

account for the relatively low scores compared to when ice is refreezing. Excluding this initialization period may give a better sense of the true performance of the simulation during this time.

For all comparisons with buoys the direction error slope is near constant. This behavior is interpreted as an indication that the model has an error which affects direction and we investigated a potential simple cause: the wind turning angle. We find in Section 4.6 that the simulation with wind turning angle 0.5 rad performs worse than those with wind turning angles of 0 and -0.5 rad. Even though there is an improvement with the modified turning angle, the metric scores are still low. These low scores lead us to examine other possible causes of direction error. Many factors can impact this metric, and in looking at drag coefficients we find that the model does not treat this effect correctly and plan on redoing the analysis once a fix is implemented.

In the definitions of the metrics in [10] and [5] we find that both biased and unbiased measures of sample variance are used. Whether this is done intentionally is unknown. However, sample sizes are large for the comparisons and so the unbiased and biased measures should be close.

All distances in the comparisons are calculated in stereographially projected, two-dimensional space. In order to ensure that the projection choice does not significantly affect the distance, several forecast comparisons are made by calculating the great-circle distance traveled by observation and simulation points using latitude and longitude data, assuming a fixed radius for the Earth. Though great-circle distance correlation and regression slope differ slightly for longer forecast lengths, the overall analysis results are similar. For the present we assume the distance calculation does not induce significant errors.

The same metrics considered in this work have been applied in the comparison of

Metric	Score
ρ_v^2	1.573
ρ	0.874
m	~ 0.6
θ_{err} (rad)	1.222
R_{err} (km)	> 10

Table 5.1: Best scores from the comparison of two different sea ice simulations with buoys. Scores are found to be consistent with the comparison of buoys and MPM_ice.

simulations using two free-drift sea ice models to buoys [9], [10]. Compared were daily displacements for each month from Jan 1995 to April 2013, as well as comparisons of variable forecast length from 1998 to 2007. The scores from these comparisons are similar to the scores found in the comparison of buoys with MPM_ice. Table 5.1 lists the best scores from the comparison of free-drift sea ice simulations with buoys. Scores from the comparisons in [10] are generally worse than those shown in Table 5.1 and become worse with increasing forecast length. MPM_ice is performing somewhat better than the free drift models and will hopefully improve further with corrections made to the implementation of the method.

The next steps in the performance validation of MPM_ice should include the examination of specific regions in the Arctic. In general, ice displacement is much larger in areas such as the Fram Strait and Bering Strait where ice is being exported from the Arctic and into the open ocean. While in the center of the Arctic ocean, away from land, displacements are generally much smaller. It is important to verify this behavior is captured by the simulation.

Chapter 6

Conclusions

This work investigates the potential of the 5 metrics presented in [10] (error radius, RMS direction error, distance regression slope, distance correlation, and vector correlation) in validating simulated sea ice displacements using the model MPM_ice [22], [21]. Using IABP buoy positions as observation, simulation displacements are compared for forecast lengths from one to thirty days. Additionally, we compare averaged daily displacements using processed RGPS satellite data for each month of 2001 and 2003. In general, the metrics show that the simulation performs relatively better for winter months.

The metrics on their own do not provide a complete picture of a model's performance. We find that frequency diagrams for displacement directions and magnitudes provide additional qualitative information for the interpretation of distance correlation and correlation coefficient, and direction error. Specifically, the distribution of direction magnitudes helps to interpret distance correlation and correlation magnitude, while the distribution of angles informs the interpretation of direction error. We also find that including displacements of 0, and the metrics' sensitivity to the number of data points being compared can lead to misleading scores.

Consistently low direction error scores led us to investigate model components that can affect displacement directions such as the wind turning angle. We ran and compared simulations using two different values for this parameter, 0 and 0.5 rad, and both led to better metric scores. The process of applying and analyzing the metrics has so far surfaced two problems in the simulation, and though the metric scores do not point directly to the cause of the problem, they provide a clue as to what might be the cause.

Appendix A

Matlab codes

A.1 Metrics

The following functions are numerical implementations of the five displacement metrics and take as their arguments vectors containing the u and v displacement vector components for both observation and simulation and return the respective metric score.

A.1.1 Distance correlation

```
%Author: Bryan McCormick (bmccormi@unm.edu)

%This function produces a regression line based on the magnitude of
%displacement vectors from observation data and material points from
%the Arctic simulation. Here the dependent variable is the material point
%displacements, the explanatory variable the observed displacements.
%Also calculated is the correlation coefficient, a number between -1 and 1
%to represent the linear dependance of the displacements.

%Inputs:
%       u1 = observation x-direction displacement
%       v1 = observation y-direction displacement
%       u2 = simulation x-direction displacement
%       v2 = simulation y-direction displacement
%Outputs:
```

```
%       corr = two dimensional vector containing the correlation
%              coefficient and the regression slope

% distance correlation
% linear regression of magnitude of displacement vectors
function corr = Distance_Correlation(u1,v1,u2,v2)

    n = length(u1);

    % get the magnitudes (distance)
    X = sqrt(u1.^2 + v1.^2);
    Y = sqrt(u2.^2 + v2.^2);

    % means
    X_bar = 1/n*(sum(X));
    Y_bar = 1/n*(sum(Y));

    % regression line
    % slope
    m = (sum(X.*Y) - n*X_bar*Y_bar)/(sum(X.*X) - n*X_bar*X_bar);

    % intercept
    b = Y_bar - m*X_bar;

    % correlation coefficient
    corr(1) = (sum(X.*Y) - n*X_bar*Y_bar)/(sqrt(sum(X.*X) - n*X_bar*X_bar)...
        *sqrt(sum(Y.*Y) - n*Y_bar*Y_bar));
    corr(2) = m;
end
```

A.1.2 Error radius

```
%Author: Bryan McCormick (bmccormi@unm.edu)

%This function measures the straight line distance between 2 points in
%kilometers. This is interpreted as the dicrepency between where a
%point was forecast to move by the Arctic simulation, and where the point
%actually went according to observation data.

%All units kilometers

%Inputs:
%       u1 = observation x-direction displacement
%       v1 = observation y-direction displacement
%       u2 = simulation x-direction displacement
%       v2 = simulation y-direction displacement
%Output:
%       Erad = average of error-radii for all buoys and material points for
%              one forecast period.

% error radius
function Erad = Error_Radius(u1,v1,u2,v2)
    n = length(u1);

    % compute the error radii
    Erad = sum(sqrt((u1 - u2).^2 + (v1 - v2).^2))/n;
```

```
end
```

A.1.3 Direction error

```
%Author: Bryan McCormick (bmccormi@unm.edu)

%This function computes the root mean square error between directions of
%observation and simulation displacement vectors. The
%direction is taken to be the angle of displacement vectors when plotted on
%the origion in radians.

%Inputs:
%       u1 = observation x-direction displacement
%       v1 = observation y-direction displacement
%       u2 = simulation x-direction displacement
%       v2 = simulation y-direction displacement
%Output:
%       RMSDE = root mean square direction error

% root mean square direction error
function RMSDE = RMS_Direction_Error(u1,v1,u2,v2)
    n = length(u1);

    % compute direction error
    RMSDE = sqrt(sum((atan2(u1.*v2 - v1.*u2,u1.*u2 + v1.*v2)).^2)/n);
end
```

A.1.4 Vector correlation

```
%Author: Bryan McCormick (bmccormi@unm.edu)

%This function is an implementation of the definition of vector correlation
%originally proposed by Hooper (1959) and suggested as a metric for sea ice
%drift model verification by Grumbine (2013). The function takes observation
%displacement vectors [u1,v1] and forecastdisplacement vectors [u2,v2]
%material points from Arctic simulation.
%Here vectorcorrelation is defined as the trace of the matrix product:
%
%S(1,1)^-1*S(1,2)*(S(2,2)^-1)*S(2,1)
%
%S(i,j) are covariance matrices between vectors ui, vj.
%See Crosby (1993) 'A Proposed Definition for Vector Correlation in
%Geophysics' for more information.

%Inputs:
%       u1 = observation x-direction displacement
%       v1 = observation y-direction displacement
%       u2 = simulation x-direction displacement
%       v2 = simulation y-direction displacement
%Output:
%       vector_Corr = number between 0 and 2 representing two dimensional
%                     correlation, 0 = no correlation, 2 = 'perfect'
%                     correlation
```

```
% function to compute correlation between 2 sets of vectors
function vector_Corr = Vector_Correlation(u1,v1,u2,v2)

    vector_Corr = VecCor(u1,v1,u2,v2);

end

%Author: Bryan McCormick (bmccormi@unm.edu)

%This function computes the squared vector correlation coefficient between
%vectors (u1,v1) and (u2,v2).
%Inputs:
%       u1 = buoy x-direction displacement
%       v1 = buoy y-direction displacement
%       u2 = material point x-direction displacement
%       v2 = material point y-direction displacement
%Output:
%       vector_Corr = number between 0 and 2 representing two dimensional
%                     correlation, 0 = no correlation, 2 = 'perfect'
%                     correlation

function ro2 = VecCor(u1,v1,u2,v2)
    f = Vecvariance(u1,u1)*(Vecvariance(u2,u2)*((Vecvariance(v1,v2)).^2)...
        + Vecvariance(v2,v2)*(Vecvariance(v1,u2)).^2)...
        +    Vecvariance(v1,v1)*(Vecvariance(u2,u2)*(Vecvariance(u1,v2).^2)...
        + Vecvariance(v2,v2)*(Vecvariance(u1,u2)).^2)...
        + 2*(Vecvariance(u1,v1)*Vecvariance(u1,v2)*Vecvariance(v1,u2)*Vecvariance(u2,v2)...
        +    Vecvariance(u1,v1)*Vecvariance(u1,u2)*Vecvariance(v1,v2)*Vecvariance(u2,v2))...
        - 2*(Vecvariance(u1,u1)*Vecvariance(v1,u2)*Vecvariance(v1,v2)*Vecvariance(u2,v2)...
        +    Vecvariance(v1,v1)*Vecvariance(u1,u2)*Vecvariance(u1,v2)*Vecvariance(u2,v2)...
        +    Vecvariance(u2,u2)*Vecvariance(u1,v1)*Vecvariance(u1,v2)*Vecvariance(v1,v2)...
        +    Vecvariance(v2,v2)*Vecvariance(u1,v1)*Vecvariance(u1,u2)*Vecvariance(v1,u2));

    g = (Vecvariance(u1,u1)*Vecvariance(v1,v1) - (Vecvariance(u1,v1).^2))...
        *(Vecvariance(u2,u2)*Vecvariance(v2,v2) - (Vecvariance(u2,v2).^2));

    ro2 = f/g;
end
```

A.2 Buoy comparison

The script MP_ComparisonConfig sets the parameters for MP_DisplacementCompare which executes the comparison between IABP buoys and simulation displacements. The script BuoySort sorts buoy position data by day.

A.2.1 MP_ComparisonConfig

```
%Author: Bryan McCormick (bmccormi@unm.edu)
%
%This script sets parameters for the script ForecastCompare. Comparison can
%be made using International Arctic Buoy Program drifting buoy
%location data.
%For a comparison over a specific region of the arctic, set Region = true

%set year for comparison
YEAR        = 2003;
month_start = 1;
month_end   = 3;

year = num2str(YEAR);
%specific region info. Set Region = 'true' to set specific region for
%comparison. Otherwise script will run for all available data.

Region = false;

%location of buoy location file
%Folder name should end with /
Buoy_folder = '~/Desktop/BuoyData/';
Buoy_file   = ['C' year];

%enter forecast length as an integer, or a vector if comparing several
%forecast lengths

%NOTE: for monthly buoy comparison FORECAST should be length 1
FORECAST = [1,5,8];

%Model Data file
%Folder name should end with /
M_folder = ['/Volumes/Icarus/MP_data/' year '/'];
M_file   = 'pmpart.nc';
```

A.2.2 BuoySort

```
%Author: Bryan McCormick (bmccormi@unm.edu)

%This function sorts IABP drifting buoy data available from NSIDC. The
%input parameter 'file' should be of the form 'Cyear' as location data is
%stored in a file named 'C'.
%The output is a cell for each day of the year containing buoy
%identification numbers and projected (x,y) location data.
%Inputs:
%   folder   - path to buoy data folder
%   file     - file for desired year
%   leapYear - logical
%Outputs:
%   BuoyData - cell containing location data sorted by day

%function to sort buoy data
function BuoyData = BuoySort(folder, file,leapYear)

    fname = [folder file];
    fID = fopen(fname);
    clear folder file fname

    %no header in file, columns as follows
    % 1) year
    % 2) month
    % 3) day
    % 4) hour in GMT (0 or 12)
    % 5) buoy identification number
    % 6) latitude in degrees north
    % 7) longitude in degrees east

    data = textscan(fID,'%d %d %d %d %d %f %f');
    fclose(fID);
    clear fID

    [X,Y] = polarstereo_fwd(data{6},data{7},6378137,0.081816153,70,-45);
    X = 1e-3*X;
    Y = 1e-3*Y;

    %sort by time of day measurements are taken
    count = 0;
    for i = 1:length(data{4})
        if data{4}(i) == 12
            count = count + 1;
            month(count)          = data{2}(i);
            day(count)            = data{3}(i);
            buoyID(count)         = data{5}(i);
            buoyLocation(count,:) = [X(i),Y(i)];
        end
    end
    clear count data X Y i

    n = length(day);
    dayNumber = zeros(1,n);
    for i = 1:n
        dayNumber(i) = month2num(day(i),month(i),leapYear);
```

```
    end
    clear day month n i

    days = unique(dayNumber);
    n = length(days);
    m = length(dayNumber);
    BuoyData = cell(n,3);

    for i = 1:n
        count = 0;
        for j = 1:m
            if dayNumber(j) == days(i)
                count = count + 1;
                BuoyData{i,1}(count) = buoyID(j);
                BuoyData{i,2}(count) = buoyLocation(j,1);
                BuoyData{i,3}(count) = buoyLocation(j,2);
            end
            if dayNumber(j) < days(i)
                continue
            end
        end
    end
    clear i j m n count
    clear days buoyID buoyLocation dayNumber

end
```

A.2.3 MP_DisplacementCompare

```
%Author: Bryan McCormick (bmccormi@unm.edu)

%This script runs a displacement comparison between material point sea ice
%model and, and IABP drifting buoy displacement data. Before running this script
%set parameters and paths to simulation and observation data in the
%MP_ComparisonConfig configuration file.

%%%%%%%%%%%%%%%%%%%%%%%%%%%%%%%%%%%%%%%%%%%%%%%%%%%%%%%%%%%%%%%%%%%%%%%%%%%%%%%%
%comparison of observation data and sea ice model
%%%%%%%%%%%%%%%%%%%%%%%%%%%%%%%%%%%%%%%%%%%%%%%%%%%%%%%%%%%%%%%%%%%%%%%%%%%%%%%%
close all
clear all

MonthStrings = ['Jan ','Feb ','Mar ','Apr ','May ','Jun',...
    'Jul ','Aug ','Sep ','Oct ','Nov ','Dec '];
MP_ComparisonConfig

%MP model data
MPfile = [M_folder M_file];
clear M_folder M_file

day_start   = 1; %starting day

%user region info
if Region == true
    figure()
    landmask
```

```
    title('choose 4 points to generate area for comparison')
    [regionX,regionY] = ginput(4);
    regionX = round(regionX);
    regionY = round(regionY);

    Xmin = min(regionX);
    Xmax = max(regionX);

    Ymin = min(regionY);
    Ymax = max(regionY);
    close all
end

%initialize buoy and material point displacement vectors
U1_buoy = [];
V1_buoy = [];
BX0     = [];
BY0     = [];
U2_B    = [];
V2_B    = [];
MX0_B   = [];
MY0_B   = [];

%check dates
leapYear = false;
if mod(YEAR,4) == 0
    leapYear = true;
end

%earth radius
REARTH = 6731;

%model data file
ncid       = netcdf.open(MPfile,'NOWRITE');

%blocktime and blocksize
varid      = netcdf.inqVarID(ncid,'blocktime');
blocktime  = netcdf.getVar(ncid,varid);
varid      = netcdf.inqVarID(ncid,'blocksize');
Blocksize  = netcdf.getVar(ncid,varid);
region     = netcdf.inqVarID(ncid,'region');

day    = unique(blocktime)/86400;
ndays  = length(day);

%mp positions and ID's
xmpID  = netcdf.inqVarID(ncid,'xMP');
mpIDs  = netcdf.inqVarID(ncid,'idMP');

%starting positions for book keeping
mpX0 = netcdf.inqVarID(ncid,'x0MP');


%%%%%%%%%%%%%%%%%%%%%%%%%%%%%%%%%%%%%%%%%%%%%%%%%%%%%%%%%%%%%%%%%%%%%%%%%%%%%%%
%Buoy comparison
%%%%%%%%%%%%%%%%%%%%%%%%%%%%%%%%%%%%%%%%%%%%%%%%%%%%%%%%%%%%%%%%%%%%%%%%%%%%%%%
BuoyData = BuoySort(Buoy_folder,Buoy_file,leapYear);
```

```
clear Buoy_folder Buoy_file

Bloopcount = 0;
figure()
for forecast = FORECAST
    %setting the forecast length and end day
    Bloopcount = Bloopcount + 1;
    Fcast(Bloopcount) = forecast;
    if month_end == 2
        if leapYear == true
            DAY = 29;
        else
            DAY = 28;
        end
    elseif month_end == 1||3||5||7||8||10||12
        DAY = 31;
    elseif month_end == 4||6||9||11
        DAY = 30;
    end

    day_end = DAY - forecast;
    if day_end <= 0
            month_end = month_end - 1;
        if month_end == 2
            if leapYear == true
                DAY_end = 29;
            else
                DAY_end = 28;
            end
        elseif month_end == 1||3||5||7||8||10||12
            DAY_end = 31;
        elseif month_end == 4||6||9||11
            DAY_end = 30;
        end
    day_end = day_end + DAY_end;

    end
    clear DAY
    %loop parameters
    numStart = month2num(day_start, month_start,leapYear);
    numEnd   = month2num(day_end, month_end,leapYear);


    %%%%%%%%%%%%%%%%%%%%%%%%%%%%%%%%%%%%%%%%%%%%%%%%%%%%%%%%%%%%
    %start forecast loop
    %%%%%%%%%%%%%%%%%%%%%%%%%%%%%%%%%%%%%%%%%%%%%%%%%%%%%%%%%%%%

    for D = numStart:numEnd
        if D + forecast > 365
            continue
        end

        dateStart = num2month(D,leapYear);
        dateEnd   = num2month(D + forecast,leapYear);

        MONTH_start = dateStart(2);
        MONTH_end   = dateEnd(2);
```

```
DAY_start    = dateStart(1);
DAY_end      = dateEnd(1);

DAYstart = month2num(DAY_start, MONTH_start,leapYear);
DAYend = month2num(DAY_end, MONTH_end,leapYear);


%%%%%%%%%%%%%%%%%%%%%%%%%%%%%%%%%%%%%%%%%%%%%%%%%%%%%%%%%%%%%%%%%%%%%%%%%%%%%%%
%get first material point blocks
blocksize = Blocksize(1);

start_blocks  = find(blocktime/86400 == day(DAYstart));
Nstart_blocks = length(start_blocks);

MP_start     = zeros(2,blocksize,Nstart_blocks);
MPx0_Start   = zeros(2,blocksize,Nstart_blocks);
start_region = zeros(blocksize, Nstart_blocks);
MPid_Start   = zeros(blocksize,Nstart_blocks,1);

start = [0, 0, start_blocks(1) - 1];
count = [2,blocksize, Nstart_blocks];

MP_start(1:2, 1:blocksize, 1:Nstart_blocks)    =...
    netcdf.getVar(ncid, xmpID, start, count)*1e-3;
MPx0_Start(1:2, 1:blocksize, 1:Nstart_blocks) =...
    netcdf.getVar(ncid, mpX0, start, count)*1e-3;
start_region(1:blocksize, 1:Nstart_blocks)     =...
    netcdf.getVar(ncid, region,start(2:3), count(2:3));
MPid_Start(1:blocksize, 1:Nstart_blocks, 1)    =...
    netcdf.getVar(ncid, mpIDs, start,[1,blocksize,Nstart_blocks]);

start_index = find(start_region == 2);

[mpX0start,mpY0start] =...
    earthCoords(MPx0_Start(1,start_index),MPx0_Start(2,start_index));

MPid_start  = MPid_Start(start_index);
[LAT,LON]   = earthCoords(MP_start(1,start_index),MP_start(2,start_index));
[MPX0,MPY0] = proj(LAT,LON);

clear LAT LON MP_start MPx0_Start start_region start count ...
    MPid_Start start_blocks Nend_blocks


%%%%%%%%%%%%%%%%%%%%%%%%%%%%%%%%%%%%%%%%%%%%%%%%%%%%%%%%%%%%%%%%%%%%%%%%%%%%%%%
%get end blocks for material points
end_blocks  = find(blocktime/86400 == day(DAYend));
Nend_blocks = length(end_blocks);


MP_end     = zeros(2,blocksize,Nend_blocks);
MPx0_End   = zeros(2,blocksize,Nend_blocks);
end_region = zeros(blocksize, Nend_blocks);
MPid_End   = zeros(blocksize,Nend_blocks,1);

start = [0, 0, end_blocks(1) - 1];
count = [2,blocksize, Nend_blocks];
```

```
MP_end(1:2, 1:blocksize, 1:Nend_blocks)    =...
    netcdf.getVar(ncid, xmpID, start, count)*1e-3;
MPx0_End(1:2, 1:blocksize, 1:Nend_blocks) =...
    netcdf.getVar(ncid, mpX0, start, count)*1e-3;
end_region(1:blocksize, 1:Nend_blocks)     =...
    netcdf.getVar(ncid, region,start(2:3), count(2:3));
MPid_End(1:blocksize, 1:Nend_blocks, 1)    =...
    netcdf.getVar(ncid, mpIDs, start,[1,blocksize,Nend_blocks]);

end_index = find(end_region == 2);

[mpX0end,mpY0end] = earthCoords(MPx0_End(1,end_index),MPx0_End(2,end_index));

MPid_end    = MPid_End(end_index);
[LAT,LON]   = earthCoords(MP_end(1,end_index),MP_end(2,end_index));
[MPXf,MPYf] = proj(LAT,LON);
clear LAT LON MP_end MPx0_end end_region start count ...
    MPid_End end_blocks Nend_blocks numstart numend

%buoy data for start and end days
%start day
start_buoyIDs = BuoyData{DAYstart,1}(:);
end_buoyIDs   = BuoyData{DAYend,1}(:);

count = 0;
for j = 1:length(start_buoyIDs)
    for k = 1:length(end_buoyIDs)
        if start_buoyIDs(j) == end_buoyIDs(k)
            count = count + 1;
            buoyStartIndex(count) = j;
            buoyEndIndex(count)   = k;
        end
    end
end

BuoyX0 = BuoyData{DAYstart,2}(buoyStartIndex(:));
BuoyY0 = BuoyData{DAYstart,3}(buoyStartIndex(:));

BuoyXf = BuoyData{DAYend,2}(buoyEndIndex(:));
BuoyYf = BuoyData{DAYend,3}(buoyEndIndex(:));

clear buoyStartIndex buoyEndIndex

%filter by user region
if Region == true
    buoyFound = false;
    count = 0;
    for j = 1:length(BuoyX0)
        if BuoyX0(j) < Xmax && BuoyX0(j) > Xmin...
                && BuoyY0(j) < Ymax && BuoyY0(j) > Ymin
            buoyFound = true;
            count = count + 1;
            RbuoyX0(count) = BuoyX0(j);
            RbuoyY0(count) = BuoyY0(j);
            RbuoyXf(count) = BuoyXf(j);
            RbuoyYf(count) = BuoyYf(j);
        end
    end
```

```
        if buoyFound == false
            continue
        end
        clear BuoyX0 BuoyY0 BuoyXf BuoyYf count
        BuoyX0 = RbuoyX0;
        BuoyY0 = RbuoyY0;
        BuoyXf = RbuoyXf;
        BuoyYf = RbuoyYf;
    end

    BuoyXdisp = BuoyXf - BuoyX0;
    BuoyYdisp = BuoyYf - BuoyY0;
    n = length(BuoyX0);

    %find the closest material points
    MPIDs = zeros(1,n);
    MPx0 = zeros(1,n);
    MPy0 = zeros(1,n);
    MPinitialX = zeros(1,n);
    MPinitialY = zeros(1,n);

    for j = 1:length(BuoyX0)

        buoyX0 = BuoyX0(j);
        buoyY0 = BuoyY0(j);

        mark = [buoyX0,buoyY0]';
        minDist = 1e6;

        for i = 1:length(MPX0)
            distance = norm(mark - [MPX0(i),MPY0(i)]');
            if distance < minDist
                minDist = distance;
                closest = [MPX0(i),MPY0(i)]';
                found   = i;
                pointID = MPid_start(i);
                pointX0(1) = mpX0start(i);
                pointX0(2) = mpY0start(i);
            end
        end
        MPIDs(j) = pointID;
        MPx0(j) = closest(1);
        MPy0(j) = closest(2);
        MPinitialX(j) = pointX0(1);
        MPinitialY(j) = pointX0(2);
    end

    %material point end data
    MPxf = zeros(1,n);
    MPyf = zeros(1,n);
    for i = 1:n
        for j = 1:length(MPid_end)
            if MPid_end(j) == MPIDs(i) && mpX0end(j) ==...
                    MPinitialX(i) && mpY0end(j) == MPinitialY(i)
                MPxf(i) = MPXf(j);
                MPyf(i) = MPYf(j);
            end
        end
```

```
        end

        %filter melted material points
        count = 0;
        for i = 1:n
            if MPxf(i) ~= 0 && MPyf(i) ~= 0

                count = count + 1;
                bx0(count) = BuoyX0(i);
                by0(count) = BuoyY0(i);

                mx0(count) = MPx0(i);
                my0(count) = MPy0(i);

                u1(count) = BuoyXdisp(i);
                v1(count) = BuoyYdisp(i);
                u2(count) = MPxf(i) - MPx0(i);
                v2(count) = MPyf(i) - MPy0(i);
            end
        end

        %save displacement vectors
        U1_buoy = [U1_buoy,u1];
        V1_buoy = [V1_buoy,v1];
        U2_B = [U2_B,u2];
        V2_B = [V2_B,v2];
        clear u1 v1 u2 v2 BuoyXdisp BuoyYdisp MPx0 MPy0 MPxf MPyf...
            BuoyX0 BuoyXf BuoyY0 BuoyYf n MPid_start MPid_end ...
            buoyEndIndex buoyStartIndex bx0 by0 mx0 my0

    end

    %statistics
    Nobs(Bloopcount) = length(U1_buoy);
    %direction error
    dErr(Bloopcount) = RMS_Direction_Error(U1_buoy,V1_buoy,U2_B,V2_B);
    %vector correlation
    VecCor(Bloopcount) = Vector_Correlation(U1_buoy,V1_buoy,U2_B,V2_B);
    %distance correlation
    Dcor(:,Bloopcount) = Distance_Correlation(U1_buoy,V1_buoy,U2_B,V2_B);
    %error radius
    Erad(Bloopcount) = Error_Radius(U1_buoy,V1_buoy,U2_B,V2_B);
    %new statistics
    [buoylength,buoyangle,mplength,mpangle,cov] =...
        VectorStats(U1_buoy,V1_buoy,U2_B,V2_B);

    meanlengthBuoy(Bloopcount) = buoylength(1);
    meanlengthMP(Bloopcount) = mplength(1);
    SDlengthBuoy(Bloopcount)   = buoylength(2);
    SDlengthMP(Bloopcount)   = mplength(2);
    VarlengthBuoy(Bloopcount)  = buoylength(3);
    VarlengthMP(Bloopcount)  = mplength(3);
    Covlength(Bloopcount)      = cov(1);

    meanAngleBuoy(Bloopcount)  = buoyangle(1);
    meanAngleMP(Bloopcount)  = mpangle(1);
    SDAngleBuoy(Bloopcount)    = buoyangle(2);
    SDAngleMP(Bloopcount)    = mpangle(2);
```

```
VarAngleBuoy(Bloopcount)    = buoyangle(3);
VarAngleMP(Bloopcount)    = mpangle(3);
CovAngle(Bloopcount)        = cov(2);
clear buoylength buoyangle mplength mpangle cov

%mean of differences
length_obs = sqrt(U1_buoy.^2 + V1_buoy.^2);
length_for = sqrt(U2_B.^2 + V2_B.^2);
theta_obs  = atan2(U1_buoy,V1_buoy);
theta_for  = atan2(U2_B,V2_B);



figure()
subplot(2,1,1)
histogram(length_obs)
ylabel('Observation (n)','FontSize',22)
ylim([0, 1500])
set(gca,'Xticklabel',[])
subplot(2,1,2)
histogram(length_for)
ylabel('Simulation (n)','FontSize',22)
%ylim([0,3500])
xlim([0,800])
xlabel('km','FontSize',22)

figure()
subplot(1,2,1)
polarhistogram(theta_obs)
%rlim([0,0.8])
title('Observation','FontSize',22)
subplot(1,2,2)
polarhistogram(theta_for)
rlim([0,800])
title('Simulation','FontSize',22)

%supplementary figures
if forecast == 1 || forecast == 15 || forecast == 30
    figure()
    plot(length_obs,length_for,'*')
    xlabel('observation (km)')
    ylabel('simulation (km)')
    hold on
    x = min(length_obs):max(length_obs);
    b = mean(length_for) - Dcor(2,Bloopcount)*mean(length_obs);
    y = Dcor(2,Bloopcount)*x + b;
    plot(x,y,'--r')
    m = num2str(Dcor(2,Bloopcount));
    p = num2str(Dcor(1,Bloopcount));
    label = {['m = ', m],['\rho = ',p]};
    text(min(x) + 5,max(length_for) -10,label,'FontSize',18);
    if forecast == 1
        title({[MonthStrings(4*month_start - 3:4*month_start),...
            '- ',MonthStrings(4*month_end -3:4*month_end),year],...
            '1-day displacement magnitudes'})
    elseif forecast == 15
        title({[MonthStrings(4*month_start - 3:4*month_start),...
            '- ',MonthStrings(4*month_end -3:4*month_end),year],...
```

```
                '15-day displacement magnitudes'})
        else
            title({[MonthStrings(4*month_start - 3:4*month_start),...
                '- ',MonthStrings(4*month_end -3:4*month_end),year],...
                '30-day displacement magnitudes'})
        end
        clear m p x y b
    end

    length_diff = length_obs - length_for;
    theta_diff  = theta_obs - theta_for;

    LengthMeanDiff(Bloopcount) = mean(length_diff);
    AngleMeanDiff(Bloopcount)  = mean(theta_diff);
    LengthSDDiff(Bloopcount)   = std(length_diff);
    AngleSDDiff(Bloopcount)    = std(theta_diff);
    LengthDiffVar(Bloopcount)  = Vecvariance(length_diff,length_diff);
    AngleDiffVar(Bloopcount)   = Vecvariance(theta_diff,theta_diff);
    clear length_obs length_for theta_obs theta_for length_diff theta_diff

    U1_buoy = [];
    V1_buoy = [];
    U2_B = [];
    V2_B = [];
    BX0 = [];
    BY0 = [];
    MX0_B = [];
    MY0_B = [];
end

%plots for buoy comparison
figure()
subplot(3,1,1)
plot(Fcast, Dcor(1,:), ':x');
grid on
hold on
plot(Fcast,VecCor,'-o');
plot(Fcast,Dcor(2,:),'--*');
ylim([-0.5,2])
ylabel('metric score')
title('January 4-5, 2001')
legend('\rho', '\rho^2_v', 'm','Location','northwest')
legend boxoff
hold off
set(gca,'Xticklabel',[])

subplot(3,1,2)
plot(Fcast,Erad,'-x')
grid on
ylabel('R_{err} (km)')
set(gca,'Xticklabel',[])


subplot(3,1,3)
hold on

plot(Fcast(1) - 1,pi/2,'^')
plot(Fcast(1) - 1,pi/3,'^')
```

```
plot(Fcast(1) - 1,pi/6,'^')
label1 = '\pi/2';
label2 = '\pi/3';
label3 = '\pi/6';
text(Fcast(1) - .9,pi/2,label1)
text(Fcast(1) - .9,pi/3,label2)
text(Fcast(1) - .9,pi/6,label3)

grid on
plot(Fcast,dErr,'-x')
xlabel('Forecast length (days)')
ylabel('\theta_{err} (rad)')
ylim([0,pi])


%vector length statistics
xax = Fcast;
figure()
subplot(4,1,1)
plot(xax,meanlengthBuoy - meanlengthMP,':x')
ylabel('Mean (km)')
title('3 month difference of mean displacement magnitude')
set(gca,'Xticklabel',[])


subplot(4,1,2)
plot(xax,SDlengthBuoy - SDlengthMP,':x')
ylabel('Standard Deviation (km)')
set(gca,'Xticklabel',[])


subplot(4,1,3)
plot(xax,(VarlengthBuoy) - (VarlengthMP),':x')
ylabel('Variance (km^2)')
set(gca,'Xticklabel',[])


subplot(4,1,4)
plot(xax,(Covlength),'-*')
xlabel('Forecast length (days)')
ylabel('Covariance (km^2)')

%vector angle statistics
figure()
subplot(4,1,1)
plot(xax,meanAngleBuoy - meanAngleMP,':x')
ylabel('Mean (rad)')
title('3 month differences of displacement angle')
set(gca,'Xticklabel',[])

subplot(4,1,2)
plot(xax,SDAngleBuoy - SDAngleMP,':x')
ylabel('Standard deviation (rad)')
set(gca,'Xticklabel',[])


subplot(4,1,3)
plot(xax,(VarAngleBuoy) - (VarAngleMP),':x')
```

```
ylabel('Variance (rad^2)')
set(gca,'Xticklabel',[])

subplot(4,1,4)
plot(xax,(CovAngle),'-*')
xlabel('Forecast length (days)')
ylabel('Covariance (rad^2)')
```

A.3 RGPS comparison

The script MonthAvgConfig sets the parameters for the script MPmonthAvg which runs the comparison between averaged-RGPS and simulation daily averaged displacements. The function SimAvg retrieves the simulation displacement data.

A.3.1 MonthAvgConfig

```
%Author: Bryan McCormick (bmccormi@unm.edu)
%
%This script sets parameters for the script MPmonthAvg.
%YEAR is the year being compared.
%SimFolder is the path to the processed simulation displacement data file,
%note: the convention implemented in the scripts requires individual files
%containing displacements for each month, named 1-12.
%RGPS_folder is the location of the RGPS displacement data files.

%year being compared
YEAR = 2001;

%locations of observation and simulation data files
Sim_folder  = '~/Desktop/MPmonthAvg/2001a/';
RGPS_folder = '~/Desktop/RGPS/Obs/';

%produce supplementary figures for the specified month or months. SupStats
%should be a vector containing the desired months as numbers 1-12. If no
%supplementary figures are desired set SupStats = 0.
SupStats = 8;

%produce figures with mean, standard deviation, variance, and covariance of
%observation and displacement lengths and angles.
AngleStats  = false;
LengthStats = false;
```

A.3.2 MPmonthAvg

```
%Author: Bryan McCormick (bmccormi@unm.edu)

%This script runs a daily averaged displacement comparison between material point sea ice
%model and, and RGPS observation displacement data. Before running this script
%set parameters and paths to simulation and observation data in the
%MonthAvgConfig configuration file.

%%%%%%%%%%%%%%%%%%%%%%%%%%%%%%%%%%%%%%%%%%%%%%%%%%%%%%%%%%%%
%comparison of daily averaged displacements
%%%%%%%%%%%%%%%%%%%%%%%%%%%%%%%%%%%%%%%%%%%%%%%%%%%%%%%%%%%%

MonthAvgConfig
year = num2str(YEAR);

%initialize vectorrs to store metric scores
DistanceCorrelation = zeros(2,12);
VectorCorrelation   = zeros(1,12);
ErrorRadius         = zeros(1,12);
DirectionError      = zeros(1,12);

%find the minimum extent
MINmonth = 9;
[RGPS_initial,RGPS_final,~] = ReadDisplacementObs(RGPS_folder,YEAR,MINmonth);
clear RGPS_displacement
RGPS_X0 = RGPS_initial(:,1);
RGPS_Y0 = RGPS_initial(:,2);
RGPS_Xf = RGPS_final(:,1);
RGPS_Yf = RGPS_final(:,2);
clear RGPS_inital RGPS_final

%compute displacements
RGPS_U = RGPS_Xf - RGPS_X0;
RGPS_V = RGPS_Yf - RGPS_Y0;
clear RGPS_Xf RGPS_Yf

%find points corresponding to ice minimum
count = 0;
for j = 1:length(RGPS_U)
    if RGPS_U(j) ~= 0 && RGPS_V(j) ~= 0
        count = count + 1;
        MINdex(count) = j;
    end
end
clear RGPS_U RGPS_V RGPS_X0 RGPS_Y0 RGPS_Xf RGPS_Yf

%loop over each month of the year
for m = 1:12
    if m == 2
        DAY_end = 28;
    elseif m == 1||3||5||7||8||10||12
        DAY_end = 31;
    elseif m == 4||6||9||11
        DAY_end = 30;
    end
```

```
%pull observation data for the month
[RGPS_initial,RGPS_final,~] = ReadDisplacementObs(RGPS_folder,YEAR,m);
clear RGPS_displacement
RGPS_X0 = RGPS_initial(:,1);
RGPS_Y0 = RGPS_initial(:,2);
RGPS_Xf = RGPS_final(:,1);
RGPS_Yf = RGPS_final(:,2);
clear RGPS_inital RGPS_final

%compute displacements
RGPS_u = RGPS_Xf - RGPS_X0;
RGPS_v = RGPS_Yf - RGPS_Y0;
clear RGPS_Xf RGPS_Yf

%pull simulation data for the month
[MP_X0,MP_Y0,MP_u,MP_v] = SimAvg(m, Sim_folder);

%filter by ice minimum
RGPS_U = RGPS_u(MINdex);
RGPS_V = RGPS_v(MINdex);

MP_U   = MP_u(MINdex);
MP_V   = MP_v(MINdex);

%compute displacement lengths and angles
length_obs = sqrt(RGPS_U.^2 + RGPS_V.^2);
length_for = sqrt(MP_U.^2 + MP_V.^2);
theta_obs  = atan2(RGPS_U,RGPS_V);
theta_for  = atan2(MP_U,MP_V);

%statistics for lengths and angles
LengthMeanObs(m)  = mean(length_obs);
LengthMeanFor(m)  = mean(length_for);
AngleMeanObs(m)   = mean(theta_obs);
AngleMeanFor(m)   = mean(theta_for);
LengthSDObs(m)    = std(length_obs);
LengthSDFor(m)    = std(length_for);
AngleSDObs(m)     = std(theta_obs);
AngleSDFor(m)     = std(theta_for);
LengthVarObs(m)   = Vecvariance(length_obs,length_obs);
LengthVarFor(m)   = Vecvariance(length_for,length_for);
AngleVarObs(m)    = Vecvariance(theta_obs,theta_obs);
AngleVarFor(m)    = Vecvariance(theta_for,theta_for);
LengthCov(m)      = Vecvariance(length_for,length_obs);
AngleCov(m)       = Vecvariance(theta_for,theta_obs);

%compute and store metric scores for the month
VectorCorrelation(m) = Vector_Correlation(RGPS_U,RGPS_V,MP_U,MP_V);
DistanceCorrelation(:,m) = Distance_Correlation(RGPS_U,RGPS_V,MP_U,MP_V);
DirectionError(m) = RMS_Direction_Error(RGPS_U,RGPS_V,MP_U,MP_V);
ErrorRadius(m) = Error_Radius(RGPS_U,RGPS_V,MP_U,MP_V);

%check for user requested supplementary figures for the month
if SupStats ~= 0
    for j = 1:length(SupStats)
        if m == SupStats(j)
            MONTH = num2str(m);
```

```
                figure()
                subplot(2,1,1)
                histogram(length_obs, 'BinWidth', 0.5)
                %title([MONTH, '/',year,' displacement magnitudes'])
                ylabel('Observation (n)','FontSize',22)
                xlim([0,9])
                ylim([0,320])
                set(gca,'Xticklabel',[])

                subplot(2,1,2)
                histogram(length_for, 'BinWidth',0.5)
                ylabel('Simulation (n)','FontSize',22)
                ylim([0,320])
                xlim([0,9])
                xlabel('km','FontSize',22)

                figure()
                subplot(1,2,1)
                polarhistogram(theta_obs)
                %rlim([0,0.8])
                title('Observation ','FontSize',22)
                subplot(1,2,2)
                polarhistogram(theta_for)
                %rlim([0,0.8])
                title('Simulation ','FontSize',22)

                figure()
                plot(length_obs,length_for,'*')
                hold on
                xlabel('observation (km)')
                ylabel('simulation (km)')
                x = min(length_obs):max(length_obs);
                M = (sum(length_obs.*length_for) - length(length_obs)*mean(length_obs)...
                    *mean(length_for))/(sum(length_obs.*length_obs) - length(length_obs)...
                    *mean(length_obs)*mean(length_obs));
                b = mean(length_for) - M*mean(length_obs);
                y = M*x + b;
                plot(x,y,'--r')
                M = num2str(DistanceCorrelation(2,m));
                P = num2str(DistanceCorrelation(1,m));
                title([MONTH, '/',year,' displacement magnitudes'])
                label = {['m = ', M],['\rho = ',P]};
                text(min(x) + .5,max(length_for) - 1,label,'FontSize',18);
                hold off
            end
        end
    end


    clear length_obs length_for theta_obs theta_for
    clear RGPS_X0 RGPS_Y0 RGPS_U RGPS_V MP_X0 MP_Y0 MP_U MP_V x10 y10 x20 y20
end

%plot the metric scores
x = 1:12;
figure()
subplot(5,1,1)
plot(x, DistanceCorrelation(1,:),'b');
```

```
ylabel('\rho','FontSize',22)
title('2003 metrics')
set(gca,'Xticklabel',[])

subplot(5,1,2)
plot(x,VectorCorrelation,'b');
ylabel('\rho^2_v','FontSize',22)
set(gca,'Xticklabel',[])

subplot(5,1,3)
plot(x,DistanceCorrelation(2,:),'b');
ylabel('m','FontSize',22)
ylim([-0.2,2])
set(gca,'Xticklabel',[])

subplot(5,1,4)
plot(x,ErrorRadius,'b')
ylabel('R_{err} (km)','FontSize',22)
set(gca,'Xticklabel',[])


subplot(5,1,5)
plot(x,DirectionError,'b')
ylabel('\theta_{err} (rad)','FontSize',22)
set(gca,'xtick',1:12,...
 'xticklabel',{'Jan','Feb','Mar','Apr','May','Jun','Jul','Aug','Sep','Oct','Nov','Dec'})

%plot the length data
if LengthStats == true
    figure()
    subplot(4,1,1)
    plot(xax,LengthMeanObs,'b')
    hold on
    plot(xax,LengthMeanFor,'r')
    ylabel('\mu (km)','FontSize',22)
    legend('obs','sim')
    legend boxoff
    title('2003 displacement magnitude')
    set(gca,'Xticklabel',[])


    subplot(4,1,2)
    plot(xax,LengthSDObs,'b')
    hold on
    plot(xax,LengthSDFor,'r')
    ylabel('s (km)','FontSize',22)
    legend('obs','sim')
    legend boxoff
    set(gca,'Xticklabel',[])


    subplot(4,1,3)
    plot(xax,LengthVarObs,'b')
    hold on
    plot(xax,LengthVarFor,'r')
    legend('obs','sim')
    legend boxoff
    ylabel('\sigma (km^2)','FontSize',22)
```

```
    set(gca,'Xticklabel',[])

    subplot(4,1,4)
    plot(xax,LengthCov)
    set(gca,'xtick',1:12,...
     'xticklabel',{'Jan','Feb','Mar','Apr','May','Jun','Jul','Aug','Sep','Oct','Nov','Dec'})
    ylabel('c (km^2)','FontSize',22)
end


%plot the angle data
if AngleStats == true
    figure()
    subplot(4,1,1)
    plot(xax,AngleMeanObs,'b')
    hold on
    plot(xax,AngleMeanFor,'r')
    ylabel('\mu (rad)','FontSize',22)
    legend('obs','sim')
    legend boxoff
    title('2003 displacement angle')
    set(gca,'Xticklabel',[])


    subplot(4,1,2)
    plot(xax,AngleSDObs,'b')
    hold on
    plot(xax,AngleSDFor,'r')
    ylabel('s (rad)','FontSize',22)
    legend('obs','sim')
    legend boxoff
    set(gca,'Xticklabel',[])


    subplot(4,1,3)
    plot(xax,AngleVarObs,'b')
    hold on
    plot(xax,AngleVarFor,'r')
    legend('obs','sim')
    legend boxoff
    ylabel('\sigma (rad^2)','FontSize',22)
    set(gca,'Xticklabel',[])

    subplot(4,1,4)
    plot(xax,AngleCov)
    set(gca,'xtick',1:12,...
     'xticklabel',{'Jan','Feb','Mar','Apr','May','Jun','Jul','Aug','Sep','Oct','Nov','Dec'})
    ylabel('c (rad^2)','FontSize',22)
end
```

A.3.3 SimAvg

```
%Author: Bryan McCormick (bmccormi@unm.edu)
%This function reads daily averaged and gridded simulation displacement
%data specified in the 'SimFile', note this function requires
%pre-processing of simulation displacement data.
%
%Inputs:
%   month   - Month of the year specified by MPmonthAvg script
%   SimFile - Location of simulation data file
%Outputs:
%   x0 - vector containing simulation initial x position
%   y0 - vector containing simulation initial y position
%   u  - vector containing simulation x displacement
%   v  - vector containing simulation y displacement

function [x0,y0,u,v] = SimAvg(month, SimFile)
    month = num2str(month);
    address = [SimFile, month];

    fID = fopen(address);
    clear address

    data = textscan(fID,'%f %f %f %f');
    x0 = data{1};
    y0 = data{2};
    u  = data{3};
    v  = data{4};
end
```

References

[1] A. Adcroft, J.-M. Campin, S. Dutkiewicz, C. Evangelinos, D. Ferreira, G. Forget, B. Fox-Kemper, P. Heimbach, C. Hill, E. Hill, H. Hill, O. Jahn, M. Losch, J. Marshall, G. Maze, D. Menemenlis, and A. Molod. *MITGCM User Manual*. Massachusetts Institute of Technology.

[2] F. I. Badgley. Heat balance at the surface of the Arctic Ocean. Proc 29th Annual Western Snow Conference Spokane, WA. PP101-104, April 1961.

[3] R. Barry, M. Serreze, J. Maslanik, and R. Preller. The Arctic Sea Ice-Climate Sytem: Observations and Modeling. *Reviews of Geophysics*, 31(4):397–422, November 1993.

[4] M. J. Brodzik and K. W. Knowles. EASE-Grid: A Versatile Set of Equal-Area Projections and Grids, 2002.

[5] D. Crosby. A Proposed Definition for Vector Correlation in Geophysics: Theory and Application. *American Meteorological Society*, 1993.

[6] D. S. Crosby, L. C. Beaker, and W. H. Gemmill. A Definition for Vector Correlation and its Application to Marine Surface Winds. *U.S. Depatment of Commerce, Office Note 365*, June 1990.

[7] D. L. Feltham. Sea Ice Rheology. *Annual Review of Fluid Mechanics*, 40:91–112, 2008.

[8] L. Girard, S. Bouillon, J. Weiss, D. Amitrano, T. Fichefet, and V. Legat. A New Modeling Framework for Sea-Ice Mechanices Based on Elasto-Brittle Rheology. *Annals of Glaciology*, 52(57), 2011.

[9] R. W. Grumbine. Virtual Floe Ice Drift Forecast Model Intercomparison. *Weather and Forecasting*, 13:886–890, September 1998.

[10] R. W. Grumbine. Long Range Sea Ice Drift Model Verification. *NOAA/NWS/NCEP/EMC/MMAB Contribution no. 315*, 2013.

[11] W. D. Hibler. A Viscous Sea Ice Law as a Stochastic Average of Plasticity. *Journal of Geophysical Research*, 82(27):3932–3938, September 1977.

[12] W. D. Hibler. A dynamic thermodynamic sea ice model. *Journal of Physical Oceanography*, 9:815–846, 1979.

[13] E. C. Hunke and J. K. Dukwicz. An Elastic-Viscous-Plastic Model for Sea Ice Dynamics. *Journal of Physical Oceanography*, 27, September 1997.

[14] R. Kwok and G. F. Cunningham. *RADARSAT Geophysical Processor System Data User's Handbook*. National Aeronautics and National Aeronautics and Space Administration, March 2000.

[15] R. Kwok and G. F. Cunningham. Sub-Daily Sea Ice Motion and Deformation from RADARSAT Observations. *Geophysical Research Letters*, 30(23), December 2003.

[16] R. Lei, P. Heil, J. Wang, Z. Zhang, Q. Li, and N. Li. Characterization of Sea-Ice Kinematic in the Arctic Outflow Region Using Buoy Data. *Polar Research*, 35(22658), 2016.

[17] R. W. Lindsay and H. L. Stern. The RADARSAT Geophysical Processor System: Quality of Sea Ice Trajectory and Deformation Estimates. *Journal of Atmospheric and Oceanic Technology*, 20:1333– 1347, September 2003.

[18] A. H. Murphy and R. L. Winkler. A General Framework for Forecast Verification. *Monthly Weather Review*, 115, July 1987.

[19] H. L. Schreyer, D. L. Sulsky, L. B. Munday, M. D. Coon, and R. Kwok. Elastic-decohesive constitutive model for sea ice. *Journal of Geophysical Research*, 111, 2006.

[20] J. P. Snyder. Map Projections- A Working Manual. *Series: Geological Survey professional paper*, (1395):186, 1987.

[21] D. Sulsky and K. Peterson. Toward a new elastic-decohesive model of Arctic sea ice. *Physica D*, (240), 2011.

[22] D. Sulsky, H. Schreyer, K. Peterson, R. Kwok, and M. Coon. Using the material-point method to model sea ice. *Journal of Geophysical Research*, 112, 2007.

[23] X. Tao, W. Perrie, F. He, Z. Li, Y. Wenlin, and H. Yilun. Spatial and Temporal Variability of Sea Ice Deformation Rates in the Arctic Ocean by RADARSAT-1. *Science China Earth Sciences*, 60(5):858–865, May 2017.

[24] W. F. Weeks. *On Sea Ice*. University of Alaska press, 2010.

[25] A. V. Wilchinsky and D. L. Feltham. A Contimuum Anisotropic Model of Sea-Ice Dynamics. *Proceedings: Mathematical, Physical and Engineering Sciences*, 460(2047):2105–2140, May 2004.